

# The Many-to-Many Mapping Between the Concordance Correlation Coefficient, and the Mean Square Error

**Vedhas Pandit**

*Chair of Embedded Intelligence for Health Care and Wellbeing,  
University of Augsburg, Germany*

VEDHAS.PANDIT@INFORMATIK.UNI-AUGSBURG.EDU

**Björn Schuller**

*Chair of Embedded Intelligence for Health Care and Wellbeing,  
University of Augsburg, Germany  
Group on Language, Audio, and Music (GLAM),  
Imperial College London, United Kingdom*

SCHULLER@INFORMATIK.UNI-AUGSBURG.EDU

## Abstract

We derive the mapping between two of the most pervasive utility functions, the mean square error ( $MSE$ ) and the concordance correlation coefficient ( $CCC$ ,  $\rho_c$ ). Despite its drawbacks,  $MSE$  is one of the most popular performance metrics (and a loss function); along with lately  $\rho_c$  in many of the sequence prediction challenges. Despite the ever-growing simultaneous usage, e. g., inter-rater agreement, assay validation, a mapping between the two metrics is missing, till date. While minimisation of  $L_p$  norm of the errors or of its positive powers (e. g.,  $MSE$ ) is aimed at  $\rho_c$  maximisation, we *reason* the often-witnessed ineffectiveness of this popular loss function with graphical illustrations. The discovered formula uncovers not only the counterintuitive revelation that ' $MSE_1 < MSE_2$ ' does *not* imply ' $\rho_{c1} > \rho_{c2}$ ', but also provides the precise range for the  $\rho_c$  metric for a given  $MSE$ . We discover the conditions for  $\rho_c$  optimisation for a given  $MSE$ ; and as a logical next step, for a given set of errors. We generalise and discover the conditions for any given  $L_p$  norm, for an even  $p$ . We present newly discovered, albeit apparent, mathematical paradoxes. The study inspires and anticipates a growing use of  $\rho_c$ -inspired loss functions e. g.,  $|MSE/\sigma_{XY}|$ , replacing the traditional  $L_p$ -norm loss functions in multivariate regressions.

**Keywords:** Multivariate Analysis, Concordance, Correlation,  $L_p$  norms, Mapping

## 1. Introduction

The need to quantify inter-rater, inter-device or inter-method agreement arises often in almost every research field (Atkinson and Nevill, 1998; Conroy et al., 2003; Lombard et al., 2002; Deyo et al., 1991; Banerjee et al., 1999). This includes, for example, a comparison between a gold standard sequence (e. g., device measurements) against the prediction sequences from a trained machine learning model, or the annotation sequences from another independent observer.

## 1.1 Literature survey: Distance and similarity metrics

For comparisons of this type, one of the most popular distance metrics in use today is the mean square error ( $MSE$ ). It measures the average squared error, i. e., the average squared difference between the two variables (Willmott and Matsuura, 2005; Fisher et al., 1920). However,  $MSE$  requires a further magnitude comparison against the measurements themselves for any meaningful interpretation.  $MSE$ , as a utility function, has also been criticised because of the unboundedness and the convexity of the function (Berger, 2013). Furthermore, the  $MSE$  metric fails to capture correlated variations of the quantities being measured (i. e., whether a greater value of one corresponds to a greater value of the other). Carl Friedrich Gauss, who himself proposed the square of the error as a measure of loss or inaccuracy, too admitted to  $MSE$ 's shortcomings and arbitrariness (Sheynin, 1979). He defended his choice to be simply “*ein bloss auf Principen der Zweckmassigkeit basierende*” (Gauss, 1860, p. 371), or as “*an appeal to mathematical simplicity and convenience*” (Lehmann and Casella, 2006, p. 6). In summary, while popular,  $MSE$  does not serve as a standalone reliable performance metric for a good number of reasons. Other metrics based on  $L_p$  norm of the errors, e. g., mean absolute error ( $MAE$ ), too suffer from exactly the same problems.

Given the populations  $X := (x_i)_1^N$  and  $Y := (y_i)_1^N$ , we have:

$$L_p = \left[ \sum_{i=1}^N |x_i - y_i|^p \right]^{\frac{1}{p}}, \quad MSE = \frac{\sum_{i=1}^N (x_i - y_i)^2}{N} = \frac{L_2^2}{N}, \quad MAE = \frac{\sum_{i=1}^N |x_i - y_i|}{N} = \frac{L_1^1}{N}. \quad (1)$$

A quest for a summary statistic—that effectively quantifies the extent of similarity and association (i. e., dependence or joint variability) between two variables—has led researchers to invent several indices. Brockmeier et al. (2017) propose an unsupervised measure to quantify informativeness of various similarity measures when used to compute correlation matrices. For comparing the two rankings, metrics such as Kendall’s Tau (Kendall, 1938), Spearman’s rank correlation coefficient (Spearman, 1961), Quotient correlation (Zhang et al., 2008) have been devised. As for the nominal and ordinal classification tasks, Cohen’s kappa coefficient ( $\kappa$ ) (Smeeton, 1985; Galton, 1892; Cohen, 1960), intraclass correlation coefficient ( $ICC$ ) (Fisher, 1925; Koch, 1982), sequence-centric distance functions (Rieck and Laskov, 2008), separation distance and rate (Hernández-Orallo et al., 2012; Collier and Dalalyan, 2016) are some of the popular metrics. While a covariance metric quantifies correlated variations of the quantities being measured, similar to  $MSE$ , this metric too is impossible to interpret without knowing the relative magnitudes of those measurements. A normalised covariance metric, called the Pearson correlation coefficient ( $\rho$ ) (Galton, 1877a,b; Pearson, 1895), quantifies the strength of the linear relationship between two variables, ignoring the bias and the scale.  $\rho$  is the covariance of the two variables normalised by the product of their standard deviations. While there exist multiple ways to interpret  $\rho$  (Lee Rodgers and Nicewander, 1988; Taylor, 1990; Weida, 1927; Rider, 1930; Székely et al., 2007),  $\rho$  essentially represents extent of the linear relationship between two variables.

$$\therefore \rho = \frac{\text{cov}(X, Y)}{\sigma_X \sigma_Y} = \frac{\sigma_{XY}}{\sigma_X \sigma_Y} = \frac{\sum_{i=1}^n (x_i - \mu_X)(y_i - \mu_Y)}{\sqrt{\sum_{i=1}^n (x_i - \mu_X)^2} \sqrt{\sum_{i=1}^n (y_i - \mu_Y)^2}}, \quad (2)$$

$$\text{where: } \sigma_X = \sqrt{\frac{\sum_{i=1}^N (x_i - \mu_X)^2}{N}}, \quad \sigma_Y = \sqrt{\frac{\sum_{i=1}^N (y_i - \mu_Y)^2}{N}},$$

$$\mu_X = \frac{\sum_{i=1}^N x_i}{N}, \quad \mu_Y = \frac{\sum_{i=1}^N y_i}{N}, \quad \text{cov}(X, Y) = \sigma_{XY} = \frac{\sum_{i=1}^n (x_i - \mu_X)(y_i - \mu_Y)}{N}.$$

While  $\rho$  signifies a linear relationship, the  $\rho$  measure fails to quantitatively distinguish between a linear relationship and an identity relationship. The  $\rho$  measure also fails to quantitatively distinguish between the linear relationship with a constant offset, the one without any offset, and an identity relationship. In summary, it fails to capture any departure from the  $45^\circ$  (slope = 1) line, i. e., any shifts in the scale (slope) and the location (offset). Thus, while successful in capturing the precision of the linear relationship, the  $\rho$  measure completely misses out on the accuracy. The concordance correlation coefficient (*CCC* or  $\rho_c$ ) (Lin, 1989) metric goes a step further, and penalises any deviation from the identity relationship, i. e., the non-unity scaling and the non-zero bias.  $\rho_c$  is a product of  $\rho$  with the term  $C_b$  that penalises such deviations in the scale and the location (Lin, 1989). The  $C_b$  component captures the accuracy, while the  $\rho$  component represents the precision. Formally,

$$\begin{aligned}
C_b &= \frac{2}{\left(v + \frac{1}{v} + u^2\right)}, & \text{where: } v &= \frac{\sigma_X}{\sigma_Y} = \text{scale-penalty, } u = \frac{(\mu_X - \mu_Y)}{\sqrt{\sigma_X \sigma_Y}} = \text{shift-penalty.} \\
\Rightarrow C_b &= \frac{2}{\left(\frac{\sigma_X}{\sigma_Y} + \frac{\sigma_Y}{\sigma_X} + \left(\frac{\mu_X - \mu_Y}{\sqrt{\sigma_X \sigma_Y}}\right)^2\right)} & &= \frac{2\sigma_X \sigma_Y}{\sigma_X^2 + \sigma_Y^2 + (\mu_X - \mu_Y)^2}. \\
\therefore \rho_c := \rho C_b &= \frac{2\rho\sigma_X \sigma_Y}{\sigma_X^2 + \sigma_Y^2 + (\mu_X - \mu_Y)^2} & &= \frac{2\sigma_{XY}}{\sigma_X^2 + \sigma_Y^2 + (\mu_X - \mu_Y)^2}. \tag{3}
\end{aligned}$$

The concordance correlation coefficient ( $\rho_c$ ) has the following characteristics:

$$\begin{array}{llll}
-1 & \leq & -|\rho| & \leq \rho_c \leq |\rho| \leq 1, & \text{sign}(\rho_c) = \text{sign}(\rho). \\
\rho_c & = & 0 & \text{if and only if: } & \rho = 0, \text{ i. e., } \sigma_{XY} = 0. \\
\rho_c & = & \rho & \text{if and only if: } & \sigma_X = \sigma_Y \text{ and } \mu_X = \mu_Y. \\
\rho_c & = & 1 & \text{if and only if: } & \rho = 1, \quad \sigma_X = \sigma_Y \text{ and } \mu_X = \mu_Y, \\
& & \text{i. e.,} & \text{if and only if: } & x_i = y_i \quad \forall i : i \in [1, N], i \in \mathbb{N}. \\
\text{Likewise, } \rho_c & = & -1 & \text{if and only if: } & x_i = -y_i \quad \forall i : i \in [1, N], i \in \mathbb{N}.
\end{array}$$

## 1.2 Literature survey: Extensions, generalisations and criticism of $\rho_c$

The  $\rho_c$ -measure is based on the distance metric, that is the expected value of the squared difference between the two measurements  $X$  and  $Y$ . Some have extended the applicability of  $\rho_c$  to more than two measurements by proposing new reliability coefficients, e. g., the overall concordance correlation coefficient (Carrasco and Jover, 2003; Barnhart and Williamson, 2001; Barnhart et al., 2002). Likewise, a more generalised version in terms of the distance function used has also been proposed (King and Chinchilli, 2001b,a), establishing its similarities with the kappa and weighted kappa coefficients. Alternative estimators for evaluating agreement and reproducibility based on the  $\rho_c$  have also been proposed (Quan and Shih, 1996; St. Laurent, 1998). Comparing the  $\rho_c$  against the previously existing four intraclass correlation coefficients presented in (Shrout and Fleiss, 1979; McGraw and Wong, 1996), Nickerson presents a strong critique of the contributions of the  $\rho_c$ -metric in evaluating reproducibility (Nickerson, 1997). The usability and apparent paradoxes associated with the reliability coefficients have been thoroughly and vehemently debated upon (Feinstein and Cicchetti, 1990; Zhao et al., 2013; Krippendorff, 2013). However,  $\rho_c$  remains arguably one of the most popular reproducibility indices, used in a wide range of fields (Nishizuka et al., 2003; Murtaza et al., 2013; Lange et al., 1999; Ma et al., 2013; Lombard et al., 2002; Conroy et al., 2003).

### 1.3 Literature survey: Growing popularity of $\rho_c$

The popularity of the measure has encouraged researchers to publish macros and software packages likewise (Carrasco et al., 2013; Crawford et al., 2007). When it comes to instance-based ordinal classification, regression, or a sequence prediction task, the machine learning community likewise has begun adapting  $\rho_c$  as the performance measure of choice (Trigeorgis et al., 2016; Pandit et al., 2018a,b; Schmitt and Schuller, 2017). Take the case of the ‘Audio/Visual Emotion Challenges’ (AVEC) for example. The shift is noticeable, with early challenges using *RMSE* as the winning criteria, to now  $\rho_c$  in those recently held (Ringeval et al., 2015; Valstar et al., 2016; Ringeval et al., 2017, 2018a). Almost without exception, the winners of these challenges have used deep learning models – which are trained to model the input to output (the raw data or features to prediction) mapping through minimisation of a loss function (Bennett and Parrado-Hernández, 2006). A loss function nominally captures the difference between a prediction from a model and the desired output; its job, consequently, is to encourage a model to drive the prediction of the model close to the desired value. While the shift in the community to use the  $\rho_c$  measure as a performance metric is definitely underway, no attempts have been made to design a loss function specifically tailored to boost  $\rho_c$ , barring a few lone exceptions (Weninger et al., 2016; Pandit et al., 2019). A few recent studies highlight the deterioration of performance through use of inconsistent loss functions (i.e., different from the performance metric), and advocate use of a consistent loss function (Pandit et al., 2019; Atmaja and Akagi, 2020; Trigeorgis et al., 2016). Yet, none provides a mathematically rigorous *reasoning* for this often-witnessed phenomenon.

The loss function used in Weninger et al., 2016; Trigeorgis et al., 2016 is directly the  $\rho_c$ , which is computationally expensive to use at every training step. This is because, the computation of  $\rho_c$  necessitates computation of standard deviations of the gold standard and the prediction, covariance between the gold standard and the prediction, the difference between the mean values at every iteration, and latter operations such as squaring, summing, and the division. Also, with  $\rho_c$  as the loss function, the partial derivative of  $\rho_c$  with respect to the outputs needs to be recalculated as well, to propagate the error down to the input layers using the backpropagation algorithm in neural networks at every step in the training iteration. In this paper, we therefore identify and isolate workable lightweight functions which directly have an impact on the  $\rho_c$  metric. We achieve this by reformulating the  $\rho_c$  in terms of individual prediction errors. Recognising the terms that are affected by the error or the prediction ‘sequence’/ordering alone, we propose a family of candidate loss functions.

## 2. Main contributions and organisation of the paper

The key contribution of this paper is that it invalidates the common notion: *MSE reduction leads to  $\rho_c$  improvement*, by deriving the most crucial, yet the missing many-to-many mapping existing between  $\rho_c$  and *MSE* in Section 3. In the section next, i.e., in Section 4, we determine the conditions for  $\rho_c$  optimisation (i.e., for  $\rho_{c_{min}}$  and  $\rho_{c_{max}}$ ), for a fixed value of *MSE*, and derive the equations for both  $\rho_{c_{min}}$  and  $\rho_{c_{max}}$  as a function of *MSE*. Using these derived equations, we find the formulations for  $\rho_c$  corresponding to the optimised *MSE* for any given  $L_p$  norm in Section 5 (for any  $p \geq 2$ ). Upon establishing the fact that efforts for *MSE* minimisation do not necessarily yield a superior prediction performance in terms of  $\rho_c$  in Section 6, we generalise Section 4 to any given  $L_p$  norm value, for any  $p$  that is an even natural number in Section 7. We then optimise  $\rho_c$  for a special case of a given *MSE*; i.e., not only a fixed *MSE* or  $L_p$  norm, but also a fixed set of error values in Section 8. We supplement our findings with illustrations in

Section 8.5. Learning from these insights, we present a family of candidate loss functions in Section 9. In Section 10, we summarise our findings and present possible future research directions.

### 3. Many-to-many mapping between $MSE$ and $\rho_c$ as a general case

**Theorem 1** For a bivariate population  $X := (x_i)_1^N$ ,  $Y := (y_i)_1^N$ ,  $\rho_c = \left(1 + \frac{MSE}{2\sigma_{XY}}\right)^{-1}$ .

**Proof**

$$\sigma_X^2 + \sigma_Y^2 + (\mu_X - \mu_Y)^2 = MSE + 2\sigma_{XY} \quad \because \text{Equation (2)}.$$

Lin (2000); Lin et al. (2002) also corroborate to the equation presented above.

$$\text{Also, } \rho_c = \frac{2\sigma_{XY}}{\sigma_X^2 + \sigma_Y^2 + (\mu_X - \mu_Y)^2} \quad \because \text{Equation (3)}.$$

$$\therefore \rho_c = \frac{2\sigma_{XY}}{MSE + 2\sigma_{XY}} = \frac{1}{1 + \frac{MSE}{2\sigma_{XY}}},$$

$$\text{i. e., } \rho_c = \left(1 - \frac{MSE}{MSE + 2\sigma_{XY}}\right) = \left(1 + \frac{MSE}{2\sigma_{XY}}\right)^{-1}. \quad (4)$$

■

### 4. Why $MSE$ as a loss function fails to improve $\rho_c$

While the minimisation of  $MSE$  loss function and the maximisation of  $\rho_c$  performance metric are both directed at achieving the perfect identity relationship between the labels (i. e., the gold standard) and the predictions, efforts for the minimisation of  $MSE$  do not necessarily translate into the maximisation of  $\rho_c$ , and vice versa. In this section, we reason and prove this fact mathematically by deriving the conditions and the formulations for  $\rho_c$  optimisation at a given  $MSE$  (i. e., given the error-set  $L_2$ -norm). To this end, we find the conditions and formulations for minimum and maximum possible values of  $\rho_c$  at a given  $MSE$ , by making use of the many-to-many mapping between  $\rho_c$  and  $MSE$  we have derived in Equation (4).

#### 4.1 $\rho_c$ optimisation, given the error-set $L_2$ -norm or the $MSE$

Inspired by the discovery that the predictions with identical  $MSE$  can map to different  $\rho_c$  values, the maximum and minimum  $\rho_c$  for a constant  $MSE$  are found next. The problem statement is, thus:

Given (1) a gold standard time series,  $G := (g_i)_1^N$ , and (2) a fixed  $MSE$  value, find the set(/s) of error values  $E := (e_i)_1^N$  that achieve maximisation and minimisation of  $\rho_c$ .

**Theorem 2** For a given  $MSE$ ,  $\rho_c$  is maximised when the errors amounting to  $MSE$  are distributed in the same ratio as of the corresponding deviations of gold standard around the mean gold standard. That is,

$$\rho_{c_{max}} = \frac{2 \left(1 + \sqrt{\frac{MSE}{\sigma_G^2}}\right)}{1 + \left(1 + \sqrt{\frac{MSE}{\sigma_G^2}}\right)^2}, \quad \text{when } e_i = \left| \sqrt{\frac{MSE}{\sigma_G^2}} \right| \cdot (g_i - \mu_G), \quad \forall i : i \in [1, N], i \in \mathbb{N}. \quad (5)$$

**Proof** Let the prediction and the gold standard sequence be  $X := (x_i)_1^N$  and  $Y := (y_i)_1^N$ , not necessarily in that order. Note that, as the formula for  $\rho_c$  is symmetric with respect to  $X$  and  $Y$ . As a result, note that which variable represents what sequence does not matter, so far as  $\rho_c$  computation is concerned. Because  $\rho_c = \left(1 + \frac{MSE}{2\sigma_{XY}}\right)^{-1}$ ,  $\rho_c$  optimisation at a given  $MSE$  necessitates  $\sigma_{XY}$  optimisation.

$$\text{Let } d_i := x_i - y_i \quad \text{and} \quad \mu_D := \frac{1}{N} \sum_{i=1}^N d_i \quad \implies \quad \mu_D = \mu_X - \mu_Y, \quad MSE := \frac{1}{N} \sum_{i=1}^N d_i^2. \quad (6)$$

$$\begin{aligned} \therefore N\sigma_{XY} &= \sum_{i=1}^N (x_i - \mu_X) \cdot (y_i - \mu_Y) = \sum_{i=1}^N (y_i + d_i - \mu_Y - \mu_D) \cdot (y_i - \mu_Y), \\ &= \sum_{i=1}^N (y_i - \mu_Y)^2 + \sum_{i=1}^N d_i \cdot (y_i - \mu_Y) - \sum_{i=1}^N \mu_D \cdot (y_i - \mu_Y). \end{aligned}$$

$$\text{If } y_i - \mu_Y := y_{z_i} \implies \sum_{i=1}^N \mu_D \cdot y_{z_i} = 0 \left( \because \sum_{i=1}^N (y_i - \mu_Y) = N\mu_Y - N\mu_Y = 0 \right).$$

$$\therefore N \cdot \sigma_{XY} = \sum_{i=1}^N y_{z_i}^2 + \sum_{i=1}^N d_i y_{z_i}. \quad (7)$$

Thus, we need to maximise  $N \cdot \sigma_{XY}$  as given by Equation (7) by tuning  $D := (d_i)_1^N$ , while satisfying the condition  $\sum_{i=1}^N d_i^2 - N \cdot MSE = 0$  ( $\because$  Equation (6)). That is,

$$\begin{aligned} \text{maximise:} \quad & f(d_1, d_2, \dots, d_N) = N \cdot \sigma_{XY} = \sum_{i=1}^N y_{z_i}^2 + \sum_{i=1}^N d_i y_{z_i}, \\ \text{subject to:} \quad & g(d_1, d_2, \dots, d_N) = \sum_{i=1}^N d_i^2 - N \cdot MSE = 0. \end{aligned}$$

Auxiliary Lagrange function  $\mathcal{L}(d_1, d_2, \dots, d_N, \lambda) = f(d_1, d_2, \dots, d_N) - \lambda \cdot g(d_1, d_2, \dots, d_N)$  is given by:

$$\begin{aligned} \mathcal{L} &= \sum_{i=1}^N y_{z_i}^2 + \sum_{i=1}^N d_i y_{z_i} - \lambda \left( \sum_{i=1}^N d_i^2 - N \cdot MSE \right). \\ \therefore \nabla_{d_1, d_2, \dots, d_N, \lambda} \mathcal{L} = 0 &\Leftrightarrow \begin{cases} y_{z_i} - 2\lambda d_i = 0 & \forall i \in \mathbb{N} : i \in [1, N]. \\ \sum_{i=1}^N d_i^2 - N \cdot MSE = 0. \end{cases} \quad (8) \end{aligned}$$

$$\begin{aligned} \therefore y_{z_i} - 2\lambda d_i = 0 \quad \forall i \in \mathbb{N} : i \in [1, N] \quad \text{and} \quad & \sum_{i=1}^N d_i^2 - N \cdot MSE = 0. \\ \therefore d_i = \frac{y_{z_i}}{2\lambda} \quad \forall i \in \mathbb{N} : i \in [1, N] \quad \implies & \sum_{i=1}^N y_{z_i}^2 = 4 \cdot \lambda^2 \cdot N \cdot MSE. \end{aligned}$$

$$\therefore d_i = \pm \sqrt{\frac{N \cdot MSE}{\sum_{j=1}^N y_{z_j}^2}} \cdot y_{z_j} = \pm \sqrt{\frac{MSE}{\sigma_G^2}} \cdot y_{z_j}. \quad (9)$$

where:  $\sigma_G^2$  = standard deviation of the gold standard  $Y := \frac{1}{N} \sum_{i=1}^N (y_i - \mu_Y)^2 = \frac{1}{N} \sum_{i=1}^N y_{z_i}^2$ .

From Equation (7),  $N\sigma_{XY}$  is maximised when  $d_i$  and  $y_{z_j}$  have identical signs. That is,

$$d_i = \left| \sqrt{\frac{N \cdot MSE}{\sum_{j=1}^N y_{z_j}^2}} \right| \cdot y_{z_j} = \left| \sqrt{\frac{MSE}{\sigma_G^2}} \right| \cdot y_{z_j}$$

Thus,  $\rho_c$  is maximised when  $MSE$  is composed of the errors (i. e.,  $\{d_i\}$ ) that are equally proportional to the deviations of the gold standard from the mean value (i. e.,  $\{y_{z_i}\} := \{y_i - \mu_Y\}$ ), and are of the same sign as of that deviations (i. e., signs of  $\{y_{z_i}\}$ ) correspondingly. With the understanding that the square-root sign denotes a positive square root, from Equation (7) we have:

$$\begin{aligned} \sigma_{XY_{max}} &= \frac{1}{N} \left( \sum_{i=1}^N y_{z_i}^2 \left( 1 + \sqrt{\frac{MSE}{\sigma_G^2}} \right) \right) = \frac{1}{N} \left( N \cdot \sigma_G^2 \left( 1 + \sqrt{\frac{MSE}{\sigma_G^2}} \right) \right), \\ &= \sigma_G^2 + \sqrt{\sigma_G^2 \cdot MSE} \end{aligned}$$

Thus, from Equation (4):

$$\begin{aligned} \rho_{c_{max}} &= \left( 1 + \frac{MSE}{2 \cdot (\sigma_G^2 + \sqrt{\sigma_G^2 \cdot MSE})} \right)^{-1} = \frac{2 \cdot (\sigma_G^2 + \sqrt{\sigma_G^2 \cdot MSE})}{MSE + 2 \cdot (\sigma_G^2 + \sqrt{\sigma_G^2 \cdot MSE})}, \\ &= \frac{2 \cdot \left( 1 + \sqrt{\frac{MSE}{\sigma_G^2}} \right)}{\frac{MSE}{\sigma_G^2} + 2 \left( 1 + \sqrt{\frac{MSE}{\sigma_G^2}} \right)} = \frac{2 \left( 1 + \sqrt{\frac{MSE}{\sigma_G^2}} \right)}{1 + \left( 1 + \sqrt{\frac{MSE}{\sigma_G^2}} \right)^2}. \end{aligned}$$

■

Likewise (cf. Appendix A), the condition and formulation for  $\rho_c$  minimisation at a given  $MSE$  are presented next.

**Theorem 3** *For a given  $MSE$ ,  $\rho_c$  is minimised when the errors amounting to  $MSE$  are distributed in the same ratio as of the corresponding deviations of gold standard around the mean gold standard, with an opposite sign. That is,*

$$\rho_{c_{min}} = \frac{2 \left( 1 - \sqrt{\frac{MSE}{\sigma_G^2}} \right)}{1 + \left( 1 - \sqrt{\frac{MSE}{\sigma_G^2}} \right)^2}, \quad \text{when} \quad e_i = - \left| \sqrt{\frac{MSE}{\sigma_G^2}} \right| \cdot (g_i - \mu_G), \quad \forall i : i \in [1, N], i \in \mathbb{N}. \quad (10)$$

**Remark 4** *Thus, in a two dimensional space  $\mathbb{R}^2 := (X, Y)$ , where  $\mathbf{x} = \left| \sqrt{\frac{MSE}{\sigma_G^2}} \right|$ ,  $\mathbf{y} = \rho_c$  (cf. Figure 1),*

$$\bullet \max_{\mathbf{x}}(\mathbf{y}) := \rho_{c_{max}} = \Psi(\mathbf{x}) := \frac{2 \times (1 + \mathbf{x})}{(1 + (1 + \mathbf{x})^2)} = \Upsilon(1 + \mathbf{x}), \quad \text{and} \quad (11)$$

$$\bullet \min_{\mathbf{x}}(\mathbf{y}) := \rho_{c_{min}} = \psi(\mathbf{x}) := \frac{2 \times (1 - \mathbf{x})}{(1 + (1 - \mathbf{x})^2)} = \Upsilon(1 - \mathbf{x}), \quad \text{where} \quad \Upsilon(\mathbf{t}) := \frac{2 \times \mathbf{t}}{1 + \mathbf{t}^2}. \quad (12)$$

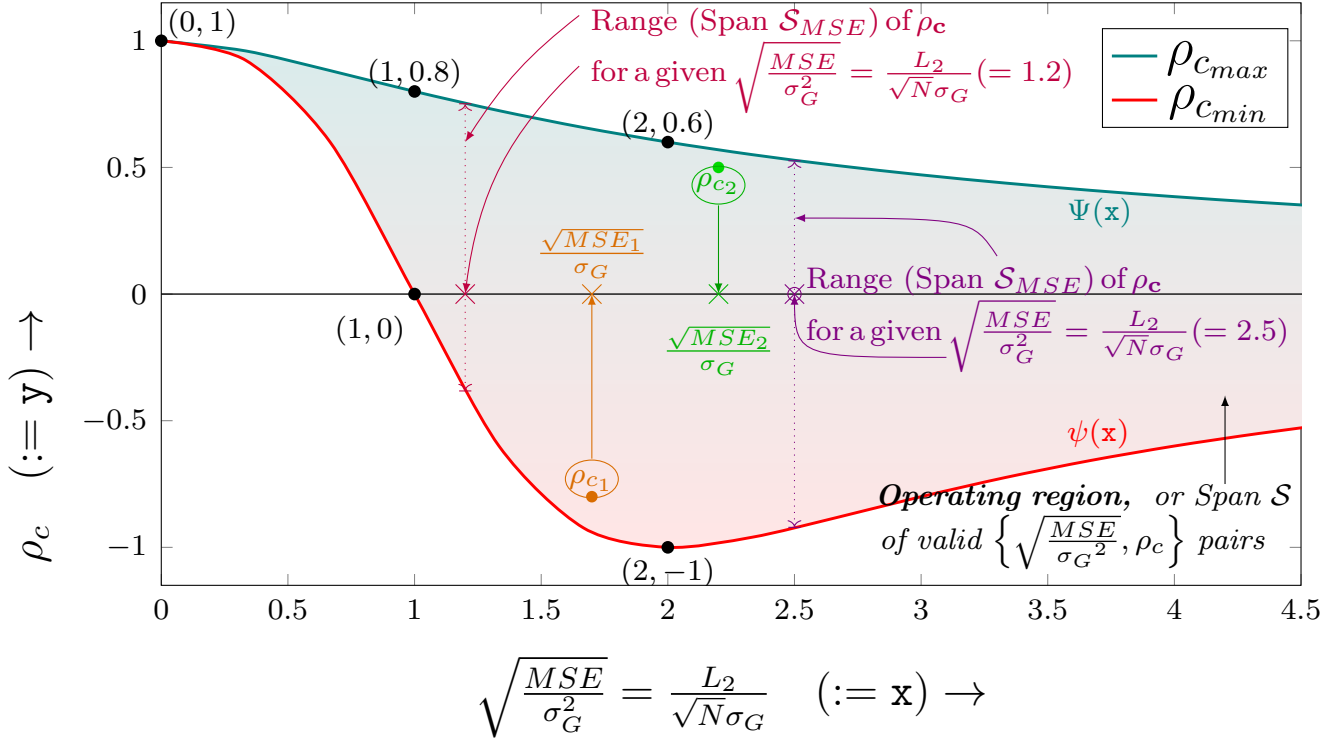


Figure 1: Range of  $\rho_c$  for a given  $MSE$  in proportion to  $\sigma_G^2$ , (i.e., to the standard deviation of the gold standard). Note that  $\rho_{c_1}$  can be  $< \rho_{c_2}$ , even though  $MSE_1 < MSE_2$ . The span  $\mathcal{S}$  of valid  $\left\{\sqrt{\frac{MSE}{\sigma_G^2}}, \rho_c\right\} = \{x, y\}$  pairs is constrained by  $\Psi(x) = \frac{2 \times (1+x)}{1+(1+x)^2}$  and  $\psi(x) = \frac{2 \times (1-x)}{1+(1-x)^2}$ .

- $\rho_{c_{min}}$  degrades to  $-1$  while  $\rho_{c_{max}}$  has only degraded to  $0.6$ . That is, while  $MSE = 0$  does translate to a perfect identity relationship, and consequently  $\rho_c = 1$ , the  $\rho_{c_{min}}$  degradation is lot quicker than that for  $\rho_{c_{max}}$  with increasing  $MSE$ .
- $\rho_{c_1} < \rho_{c_2}$  even though for the corresponding mean square errors,  $MSE_1 < MSE_2$ . That is, the  $MSE$  reduction does not automatically translate to  $\rho_c$  improvement.

In summary, as per Theorems 2 and 3, the  $\rho_c$  can vary between  $\frac{2\left(1-\sqrt{\frac{MSE}{\sigma_G^2}}\right)}{1+\left(1-\sqrt{\frac{MSE}{\sigma_G^2}}\right)^2}$  and  $\frac{2\left(1+\sqrt{\frac{MSE}{\sigma_G^2}}\right)}{1+\left(1+\sqrt{\frac{MSE}{\sigma_G^2}}\right)^2}$  for

given  $MSE$  – depending on how  $MSE$  is split into its constituent errors. For the sake of completeness, we note here that even if the constituent error-set that makes  $MSE$  is known fully,  $\rho_c$  cannot be estimated. The knowledge of not only the values of the constituent errors, but also their sequence is a prerequisite for estimating  $\rho_c$ , as we prove later in Section 8.



## 5. Why other $L_p$ -norms fail as a loss function (even more spectacularly than $MSE$ )

For error reduction, one can also use  $MAE$ , or mean ‘Mean  $k$ -Powered Error (i. e.,  $MkE^1$ ) in general instead of  $MSE$ , i. e., choosing an optimal  $k$  that could be bigger or smaller than 2.

$$\text{Because } MkE := \frac{\left(\sum_{i=1}^N |d_i|^k\right)}{N} = \frac{L_k^k}{N} \implies L_k = N^{\frac{1}{k}} \cdot MkE^{\frac{1}{k}}. \quad (13)$$

Similar to  $MSE$ , while the minimisation of  $MkE$  (i. e., minimisation of the errors) and the maximisation of  $\rho_c$  are both directed at achieving the perfect identity relationship between the labels (i. e., the gold standard) and the predictions, the efforts for minimisation of  $MkE$  do not necessarily translate into maximisation of  $\rho_c$ , and vice versa. In this section, we reason and prove this fact mathematically.

While no known direct mapping exists between  $MkE$  (for  $k \neq 2$ ) and  $\rho_c$ , the many-to-many mapping existing between  $MSE$  and  $\rho_c$  (established in Section 3), and the inequality relationship existing between  $MkE(k \neq 2)$  and  $MSE$  can be used to establish the formulations and conditions for the minimum and maximum possible values of  $\rho_c$  at the given  $MkE$ , through optimisation of  $MSE$ .

### 5.1 $\rho_c$ optimisation using $MSE$ optimisation, given the error-set $L_p$ -norm, $p > 0$

$$\text{For } 0 < r < p \text{ as per Appendix F: } L_p \leq L_r \leq N^{\frac{p-r}{pr}} L_p. \quad (14)$$

$$\therefore \text{ For } k > 2: \quad L_k \leq L_2 \leq N^{\frac{k-2}{2k}} \cdot L_k$$

$$\therefore \text{ From Equation (13): } N^{\frac{1}{k}} \cdot MkE^{\frac{1}{k}} \leq N^{\frac{1}{2}} \cdot MSE^{\frac{1}{2}} \leq N^{\frac{k-2}{2k}} N^{\frac{1}{k}} \cdot MkE^{\frac{1}{k}}.$$

$$\implies \quad N^{\frac{2-k}{2k}} \cdot MkE^{\frac{1}{k}} \leq MSE^{\frac{1}{2}} \leq MkE^{\frac{1}{k}}.$$

$$\text{i. e., } \sqrt{MSE_{min}} \leq \sqrt{MSE} = \theta \cdot \sqrt{MSE_{min}} \leq \theta_{max} \cdot \sqrt{MSE_{min}}, \quad (15)$$

$$\text{where: } \sqrt{MSE_{min}} = \frac{L_k}{\sqrt{N}} = N^{\frac{2-k}{2k}} \cdot MkE^{\frac{1}{k}}, \quad \text{and} \quad \sqrt{MSE_{max}} = \theta_{max} \cdot \sqrt{MSE_{min}},$$

$$\text{and } \theta_{min} = 1 \leq \theta := \frac{N^{\frac{1}{2}} MSE^{\frac{1}{2}}}{N^{\frac{1}{k}} MkE^{\frac{1}{k}}} \leq N^{\frac{k-2}{2k}} = \theta_{max}.$$

Similarly (cf. Appendix B), for  $k \in (0, 2)$ :

$$\sqrt{MSE_{min}} \leq \sqrt{MSE} = \theta \cdot \sqrt{MSE_{min}} \leq \theta_{max} \cdot \sqrt{MSE_{min}}, \quad (16)$$

$$\text{where: } \sqrt{MSE_{min}} = \frac{L_k}{N^{\frac{1}{k}}} = MkE^{\frac{1}{k}} \quad \text{and} \quad \sqrt{MSE_{max}} = \theta_{max} \cdot \sqrt{MSE_{min}},$$

$$\text{and } \theta_{min} = 1 \leq \theta := \frac{MSE^{\frac{1}{2}}}{MkE^{\frac{1}{k}}} \leq N^{\frac{2-k}{2k}} = \theta_{max}.$$

$$\therefore \text{ For } k = 1: \quad \sqrt{MSE_{min}} \leq \sqrt{MSE} = \theta \cdot \sqrt{MSE_{min}} \leq \theta_{max} \cdot \sqrt{MSE_{min}}, \quad (17)$$

$$\text{where: } \sqrt{MSE_{min}} = \frac{L_1}{N} = MAE \quad \text{and} \quad \sqrt{MSE_{max}} = \theta_{max} \cdot \sqrt{MSE_{min}},$$

$$\text{and } \theta_{min} = 1 \leq \theta \leq \sqrt{N} = \theta_{max}.$$

---

1. We intentionally avoid using the term  $MpE$  for ‘Mean  $p$ -Powered Error’ (although more consistent with the term  $L_p$ ), since  $MPE$  is more popularly the ‘Mean Percentage Error’ in the literature.

The lower the  $\theta$  (i.e., the lower the  $MSE$ ), the higher is the maximum theoretical limit for  $\rho_c$  at the given  $MkE$ ;  $\rho_{c_{max}}$  being a monotonic function of  $MSE$  (cf. Figure 1). However, the same cannot be said for the minimum theoretical limit for  $\rho_c$  at the given  $MkE$ , since  $\rho_{c_{min}}$  is not a monotonic function of  $MSE$  (cf. Figure 1). Notice that attaining these theoretical limits (i.e.,  $\rho_{c_{max}}$  and  $\rho_{c_{min}}$ ) is subject to also meeting simultaneously the conditions dictated by Theorems 2 and 3 at the given  $MkE$  with the given gold standard, which can not be guaranteed to be true of any gold standard as a general case. Thus, for the sake of clarity, we denote these theoretical limits at given  $L_k$  with  $\rho_{c_{max}'}$  and  $\rho_{c_{min}'}$  respectively.

$$\begin{aligned} \therefore \text{From Equation (15), for } k \geq 2: \quad \rho_{c_{max}'} &= \frac{2\left(1 + \frac{L_k}{\sqrt{N}\sigma_G}\right)}{1 + \left(1 + \frac{L_k}{\sqrt{N}\sigma_G}\right)^2} = \Psi\left(\frac{L_k}{\sqrt{N}\sigma_G}\right), \\ \text{and} \quad \rho_{c_{min}'} &= \frac{2\left(1 - \theta \frac{L_k}{\sqrt{N}\sigma_G}\right)}{1 + \left(1 - \theta \frac{L_k}{\sqrt{N}\sigma_G}\right)^2} = \psi\left(\frac{\theta \cdot L_k}{\sqrt{N}\sigma_G}\right), \theta \in \left[1, N^{\frac{k-2}{2k}}\right]. \end{aligned} \quad (18)$$

$$\text{From Equation (16), for } k \in (0, 2]: \quad \rho_{c_{max}'} = \Psi\left(\frac{L_k}{N^{\frac{1}{k}}\sigma_G}\right), \rho_{c_{min}'} = \psi\left(\frac{\theta \cdot L_k}{N^{\frac{1}{k}}\sigma_G}\right), \theta \in \left[1, N^{\frac{2-k}{2k}}\right]. \quad (19)$$

Thus, from Equations (18) and (19), irrespective of the value of  $k > 0$  (i.e., whether  $k \geq 2$  or  $k \leq 2$ ):

$$\rho_{c_{max}'} = \Psi(\mathbf{x}), \mathbf{x} \in [0, \infty), \text{ and } \rho_{c_{min}'} = \begin{cases} \psi(\theta_{max} \cdot \mathbf{x}), & \mathbf{x} \in [0, \frac{2}{\theta_{max}}]. \\ -1 = \psi(\theta_0 \cdot \mathbf{x}), & \mathbf{x} \in [\frac{2}{\theta_{max}}, 2], \quad \theta_0 := \frac{2}{\mathbf{x}}, \quad \theta_{max} := N^{\lfloor \frac{k-2}{2k} \rfloor} \\ \psi(\mathbf{x}), & \mathbf{x} \in [2, \infty). \end{cases} \quad (20)$$

in the  $\mathbb{R}^2 = \{\mathbf{X}, \mathbf{Y}\} = \left\{\frac{L_k}{\sqrt{N}\sigma_G}, \rho_c\right\}$  space for  $k \geq 2$ , and in the  $\{\mathbf{X}, \mathbf{Y}\} = \left\{\frac{L_k}{N^{\frac{1}{k}}\sigma_G}, \rho_c\right\}$  space for  $k \leq 2$ .

For the sake of completeness, we note here that the range for  $\rho_c$  at a given  $MkE$  is typically even smaller than the one dictated by Equation (20) above (as we establish later in Section 6). This is because the boundary conditions for  $\theta$  (e.g.,  $\theta = \frac{\sqrt{MSE}}{MAE} = \{1, \sqrt{N}\}$ ) are met only when the error coefficients are constant valued – either entirely, or except at one instance (Willmott and Matsuura, 2005)<sup>2</sup>. Simultaneously,  $\rho_{c_{max}'}$  and  $\rho_{c_{min}'}$  are obtained if and only if the error coefficients are in the same ratio as of the deviations of the corresponding gold standards (cf. Theorems 2 and 3), which forces the gold standard to be constant valued likewise – i.e., either entirely, or except at one instance – which is not true in general. Thus, assuming  $\rho_{c_{max}'}$  from Equation (20) to be the true maximum limit of  $\rho_c$  at any given  $L_k$  norm is equivalent of defining the gold standard to be constant-valued for at least  $N - 1$  instances.

Nonetheless, plotting the incorrect span of valid  $\{\rho_c, L_k\}$  pairs as dictated by Equation (20) gives us a few new insights still – as to how assuming even this incorrect line of argument (i.e., a more optimistic  $\rho_{c_{max}}$  as a function of  $MkE$ , and consequently,  $\rho_c$  maximisation through  $MkE$  minimisation) leads us to a more discouraging end-result to the contrary. We discuss in Section 7 the derivations for true span  $\mathcal{S}$  of valid  $\{\rho_c, L_p\}$  pairs.

---


$$\begin{aligned} \text{When } e_i = \pm e_j, \quad \forall i, j \in [1, N], \quad i, j \in \mathbb{N} &\implies MAE = |e_i|, \quad MSE = e_i^2 \implies \theta_{k=1} := \frac{\sqrt{MSE}}{MAE} = 1. \\ \text{2. When } e_j = 0, \quad \exists! i, \forall j \neq i, i, j \in [1, N], \quad i, j \in \mathbb{N} &\implies MAE = \frac{|e_i|}{N}, \quad MSE = \frac{e_i^2}{N} \implies \theta_{k=1} := \frac{\sqrt{MSE}}{MAE} = \sqrt{N}. \end{aligned}$$

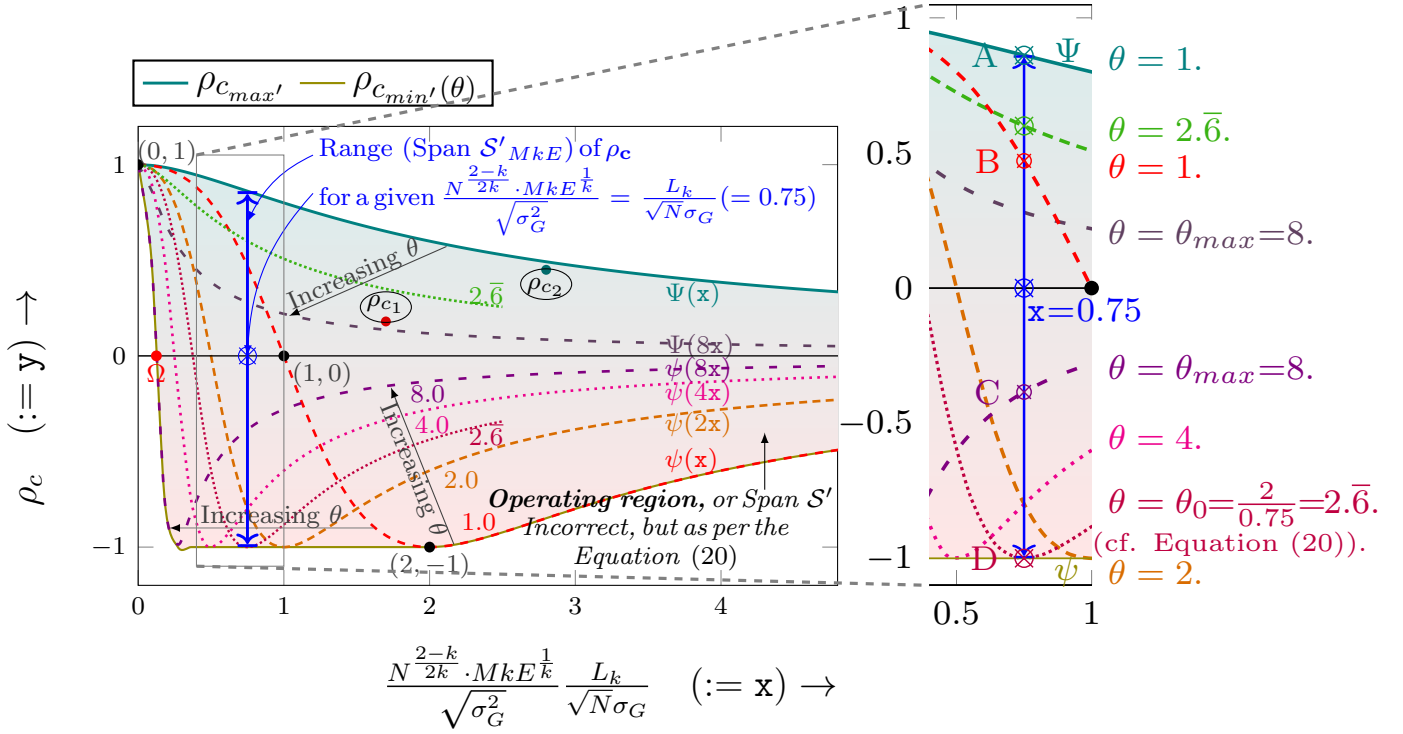


Figure 2: Range of  $\rho_c$  as per Equation (20), as a function of given  $MkE = \frac{L_k}{N}$ ,  $k > 2$  with respect to the gold standard consisting of  $N$  samples, standard deviation of  $\sigma_G^2$ ,  $1 \leq \theta \leq N^{\frac{k-2}{2k}}$ . Notice the increase in the operating region compared to Figure 1 to  $\mathcal{S}'$ , due to  $\rho_{c_{min'}} = \psi(\theta \cdot \mathbf{x})$  with increasing  $\theta$ . While each point in  $\mathcal{S}'$  maps to a unique  $\{L_k, \rho_c\}$  pair, each maps to infinitely many  $\{L_2\}$  or  $\{MSE\}$  values – except those points lying exactly on the  $\rho_{c_{max}}$   $\rho_{c_{min}}$  curves which map to only one  $MSE$ . Similar to Figure 1,  $MkE_1 \leq MkE_2$  does not guarantee  $\rho_{c_1} \leq \rho_{c_2}$ . For the sake of completeness, we note further that the true  $\rho_{c_{max}}$  and consequently, the true span  $\mathcal{S}$  is even smaller than the one shown above (cf. Section 6).

**Remark 5** Thus, for a two dimensional space  $\mathbb{R}^2 := (\mathbf{X}, \mathbf{Y})$ , where  $\mathbf{x} = \left| \frac{L_k}{\sqrt{N\sigma_G}} \right|$ ,  $\mathbf{y} = \rho_c$  (cf. Figure 2),

- While reducing  $MSE$  does not always guarantee  $\rho_c$  improvement (cf. Section 3),  $MSE$  reduction through enough number of iterations to a small enough value<sup>3</sup> guarantees a positive  $\rho_c$  nonetheless. However, a negative  $\rho_c$  remains a possibility for  $L_k$  as small as  $\frac{\sqrt{N}\sigma_G}{N^{\frac{k-2}{2k}}}$  with  $\theta = \theta_{max}$  (cf. Figure 2). While  $N$  typically is very large, even for  $N$  as small as 64 (i. e.,  $\sqrt{N} = 8$ ), this translates to the rapid deterioration of  $\rho_{c_{min}}$  from point  $(0, 1)$  to point  $\Omega$  i. e.,  $(0.125, 0)$  – as opposed to  $(1, 0)$ .
- Higher the  $N$ , more diminished is the effect of reduction of  $MkE$  in terms of improving  $\rho_c$ , i. e., quicker the deterioration of  $\rho_c$  from  $\rho_{c_{min}} = 1$ , i. e., point  $(0, 1)$  to  $\rho_{c_{min}} = -1$ .

3. That is, for  $MSE \leq \sigma_G^2$  (cf.  $\sqrt{MSE/\sigma_G^2} \in [0, 1]$  in Figure 1)

- Increase in  $N$  implies an increase in the range of valid  $\theta$  values, i. e., effectively an increase in the range of possible MSE values for any given  $L_k$ -norm.
- Increase in the range for  $\theta$  manifests into an increase in the operating region with a negative  $\rho_c$ , which asymptotically approaches the negative Y-axis.
- Consistent to findings from Section 3 and fig. 1, the reduction in MSE at a constant  $L_k$  norm (even if assumed to be achievable to its lowest limit for the given gold standard) does not always translate to improvement in  $\rho_c$ .

For example, starting with  $\theta = \theta_{max} = 8$  at a given  $\frac{L_k}{\sqrt{N}\sigma_G} (= 0.75)$ , the MSE reduction (i. e., effectively the  $\theta$  reduction) causes further deterioration of  $\rho_{c_{min}}$  to  $-1$ , i. e., when  $\theta$  becomes equal to  $\frac{2}{x} = \frac{2}{0.75} = 2.\bar{6}$  (the trajectory  $C \rightarrow D$ ). While further reduction in MSE does begin to make  $\rho_{c_{min}}$  more positive, the  $\rho_{c_{min}}$  remains overall negative until  $\theta$  is reduced to  $\frac{\theta_0}{2} = \frac{1}{x} = \frac{1}{0.75} = 1.\bar{3}$ . In summary, MSE reduction at a given  $L_p$  norm does not necessarily result in a  $\rho_c$  improvement.

- While each point in  $\mathcal{S}'$  maps to a unique  $\{L_k, \rho_c\}$  pair, each maps to infinite number of MSE values (except the points on the  $\rho_{c_{max}}$  and  $\rho_{c_{min}}$  curves which map to only one MSE, e. g., the points A and D in Figure 2). This is because, to be in  $\mathcal{S}'$ , every  $\left\{ \frac{L_k}{\sqrt{N}\sigma_G}, \rho_c \right\} \Big|_{MSE = \frac{\theta \cdot L_k}{\sqrt{N}\sigma_G}}$  needs to only satisfy the condition  $\rho_c \in \left[ \psi \left( \frac{\theta \cdot L_k}{\sqrt{N}\sigma_G} \right), \Psi \left( \frac{L_k}{\sqrt{N}\sigma_G} \right) \right]$  such that  $\theta \in [1, \theta_{max}]$ , which is true for infinite number of  $\theta$  (except the points on the  $\rho_{c_{max}}$  and  $\rho_{c_{min}}(\theta)$  plots, where  $\theta = 1$  and  $\theta = \theta_0$  only respectively, i. e., no variation in  $\theta$  is allowed).

For example, for every point on the segment AD in Figure 2,  $\frac{L_k}{\sqrt{N}\sigma_G} = 0.75$ . Thus, for every point on the segment AD where  $\rho_c < 0$  except the point D,  $\psi(\theta \times 0.75) = \rho_{c_{given}}$  has two solutions  $\theta_1$  and  $\theta_2$  that are related by an equation<sup>4</sup>:  $\theta_2 = \frac{\theta_1}{\frac{L_k}{\sqrt{N}\sigma_G} \theta_1 - 1} = \frac{\theta_1}{0.75\theta_1 - 1}$ . As an example, for the point C which is known to simultaneously lie on the curve  $\phi(\theta_{max} \times \mathbf{x}) = \phi(8 \times \mathbf{x})$ , one of the two  $\theta$  values is 8, and thus,  $\{\theta_1, \theta_2\} = \left\{ \theta_1, \frac{\theta_1}{0.75\theta_1 - 1} \right\} = \{8, 1.6\}$ . Thus,  $\rho_c|_C \in \left[ \psi \left( \frac{\theta_0 \cdot L_k}{\sqrt{N}\sigma_G} \right), \Psi \left( \frac{L_k}{\sqrt{N}\sigma_G} \right) \right]$ , i. e.,  $\psi \left( \frac{\theta_0 \cdot L_k}{\sqrt{N}\sigma_G} \right) \leq \rho_c|_C \leq \Psi \left( \frac{L_k}{\sqrt{N}\sigma_G} \right)$  is true for every value of  $\theta_0 \in [\theta_1, \theta_2] = [1.6, 8]$ . That is, while point C maps to  $\left\{ \frac{L_k}{\sqrt{N}\sigma_G} = 0.75, \rho_c = \phi(0.75 \times 8) = -0.3846 \right\}$ , it can map to  $\sqrt{MSE} \in [0.75\sigma_G \times 1.6, 0.75\sigma_G \times 8]$ , i. e.,  $1.44\sigma_G^2 \leq MSE \leq 36\sigma_G^2$ .

Identical observations can be made for  $k < 2$  as well, the only difference being  $\mathbf{x} = L_k N^{-\frac{1}{k}}$  (cf. Appendix C).

$$\begin{aligned}
4. \quad & \text{Let } \rho_c = y = \psi(\theta_1 \mathbf{x}) = \psi(\theta_2 \mathbf{x}) \quad \implies \quad \frac{2(1-\theta_1 \mathbf{x})}{1+(1-\theta_1 \mathbf{x})^2} = \frac{2(1-\theta_2 \mathbf{x})}{1+(1-\theta_2 \mathbf{x})^2}, \text{ where } \mathbf{x} = \frac{L_k}{\sqrt{N}\sigma_G}. \\
& \therefore \quad (1 - \theta_1 \mathbf{x}) + (1 - \theta_1 \mathbf{x})(1 - \theta_2 \mathbf{x})^2 = (1 - \theta_2 \mathbf{x}) + (1 - \theta_2 \mathbf{x})(1 - \theta_1 \mathbf{x})^2. \\
& \therefore \quad (1 - \theta_1 \mathbf{x})(1 - \theta_2 \mathbf{x})((1 - \theta_2 \mathbf{x}) - (1 - \theta_1 \mathbf{x})) = (1 - \theta_2 \mathbf{x}) - (1 - \theta_1 \mathbf{x}). \\
& \therefore \quad (1 - \theta_1 \mathbf{x})(1 - \theta_2 \mathbf{x}) = 1 \implies \quad \theta_1 \theta_2 \mathbf{x} = \theta_1 + \theta_2. \\
& \therefore \quad \theta_2 = \frac{\theta_1}{\mathbf{x}\theta_1 - 1}, \text{ where } \mathbf{x} = \frac{L_k}{\sqrt{N}\sigma_G}.
\end{aligned}$$

## 6. True span of valid $\{L_p, \rho_c\}$ pairs, given a gold standard sequence

In Section 5, we noted that the Equation (20) does not represent the true span of  $\rho_c$ . While the true  $\rho_{c_{max}} \leq \rho_{c_{max}'}$  always, the true  $\rho_{c_{min}} \geq \rho_{c_{min}'}$  need not necessarily be true. This is because  $\rho_{c_{max}'}|_{L_{k_{given}}}$  not only assumes that  $MSE = MSE_{min}$ , but also that the error coefficients and the corresponding deviations of the gold standard from the mean are in equal ratio (cf. Theorem 2); the two mutually contradictory assumptions in general. However, the  $\rho_{c_{min}'}(\theta)|_{L_{k_{given}}}$  is not conditioned upon  $MSE = MSE_{min}$  or  $MSE = MSE_{max}$ , but rather at some  $\theta_0 \times MSE_{min} : \exists \theta_0 \in [1, \theta_{max}]$ . Thus, the error coefficients in this case are not constrained to simultaneous assumptions that can be mutually contradictory.

Specifically, for  $k > 2$ ,  $MSE|_{L_{k_{given}}}$  is minimised to  $MSE_{min}$  *only when*<sup>5</sup> the error-set  $E$  consists of all zeros except one  $e_i = \pm N^{\frac{1}{k}} \cdot MkE^{\frac{1}{k}}, \exists i : 1 \leq i \leq N$  – thus,  $2N$  possible sequences. Likewise,  $MSE|_{L_{k_{given}}}$  is maximised (i. e.,  $MSE_{max}$ ) *only when* the  $L_p$  norm is divided into errors of equal magnitudes, i. e.,  $e_i = \pm MkE^{\frac{1}{k}}, \forall i : 1 \leq i \leq N$  – thus,  $2^N$  possible sequences. For  $k < 2$ ,  $MSE|_{L_k}$  is minimised and maximised at identically opposite conditions. Simultaneously,  $\rho_c$  optimisation in either direction requires that the magnitudes of the errors are directly proportional to the corresponding deviations of the gold standard sequence instances from the gold standard mean (cf. Theorems 2 and 3). These simultaneous conditions dictate that the gold standard is constant valued – either entirely, or except at one instance – which is not true for a gold standard as a general case. Thus, unless these conditions are satisfied for a given gold standard, the points  $A$  and  $C$  in Figure 2 map to very different values of  $L_k$ ; i. e., the two points are not attainable at a given  $L_k$ . Thus, the allowed scope of the trajectory of  $MSE$  minimisation at a given  $L_p$  norm is quite restricted compared to  $\mathcal{S}'$ . The restriction imposed (i. e., the true span  $\mathcal{S}$ ) is evidently a function of the given gold standard sequence, since that sequence alone dictates the optimised distribution and sequence of errors.

**Remark 6** Thus, for a two dimensional space  $\mathbb{R}^2 := (\mathbf{X}, \mathbf{Y})$ , where  $\mathbf{x} = \left| \frac{MSE}{\sigma_G} \right|$ ,  $\mathbf{y} = \rho_c$  (cf. Figure 3),

- There can be at the most  $2N$  and  $2^N$   $\{MSE, \rho_c\}$  pairs mapped  $\in \mathcal{S}$  at the two extremums (cf. the two blue lines in Figure 3). The example true operating region in Figure 3, therefore, does not converge to a unique point at either  $MSE$  extremum, nor can all of the infinitely many points lying on the two blue lines be part of  $\mathcal{S}$  (cf. Figure 2).
- The span rather starts and ends with at the most  $2N$  and  $2^N$  points at  $MSE_{min}$  and  $MSE_{max}$  extremum respectively for  $k > 2$  (while  $2^N$  and  $2N$  number of points respectively for  $k < 2$ ).

---


$$\begin{aligned}
 & \text{When } e_j = 0, \quad \exists! i, \forall j \neq i, i, j \in [1, N], i, j \in \mathbb{N} \implies MSE = \frac{e_i^2}{N} \quad MkE = \frac{|e_i|^k}{N} \implies \theta_{k < 2} := \frac{\sqrt{MSE}}{MkE^{\frac{1}{k}}} = \frac{N^{\frac{1}{k}}}{N^{\frac{1}{2}}} = N^{\frac{2-k}{2k}}. \\
 & \implies \theta_{k > 2} := \frac{\sqrt{MSE}}{N^{\frac{2-k}{2k}} \cdot MkE^{\frac{1}{k}}} = 1. \\
 & \text{5. When } e_i = \pm e_j, \quad \forall i, j \in [1, N], i, j \in \mathbb{N} \implies MSE = e_i^2, \quad MkE = |e_i|^k \implies \theta_{k < 2} := \frac{\sqrt{MSE}}{MkE^{\frac{1}{k}}} = 1. \\
 & \implies \theta_{k > 2} := \frac{\sqrt{MSE}}{N^{\frac{2-k}{2k}} \cdot MkE^{\frac{1}{k}}} = N^{\frac{k-2}{2k}}.
 \end{aligned}$$

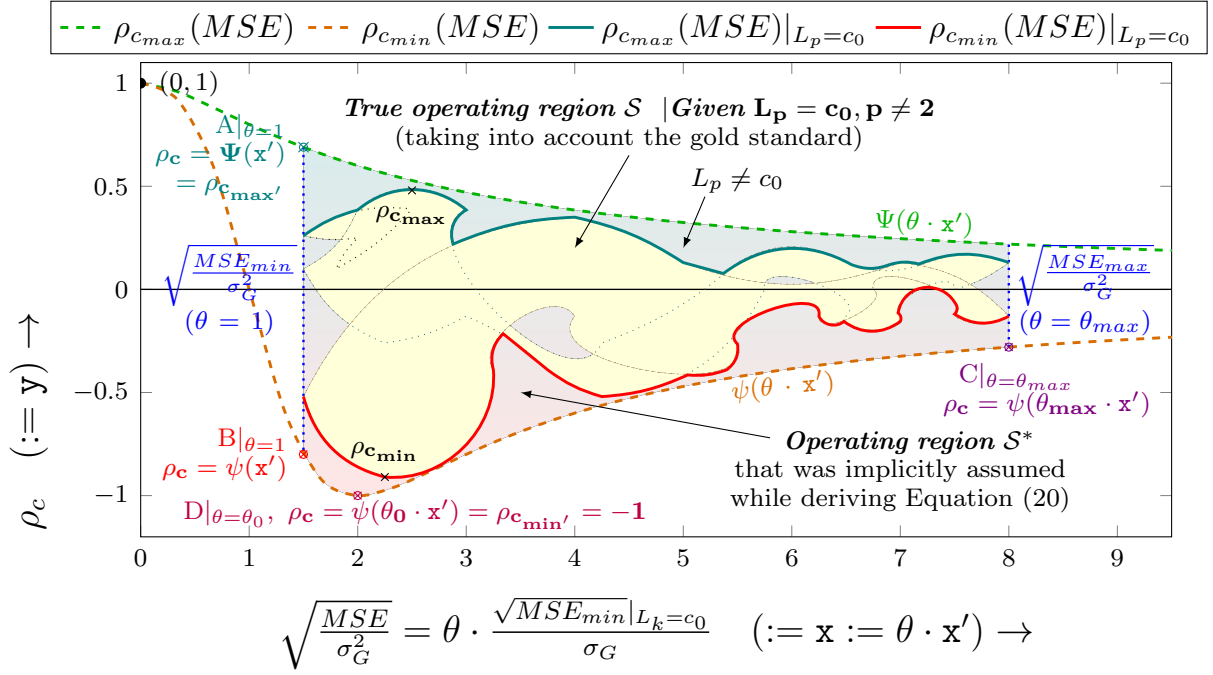


Figure 3: Comparison between the true  $\rho_{c_{min}}$  and  $\rho_{c_{max}}$  and those obtained with  $MSE$  optimisation ( $\rho_{c_{max}'}$  and  $\rho_{c_{min}'}$  using Equation (20)) for a given  $L_p = c_0$ . For  $k > 2$ ,  $MSE_{min}^{\frac{1}{2}} = N^{\frac{2-k}{2k}} \cdot Mke^{\frac{1}{k}}$  and  $MSE_{max}^{\frac{1}{2}} = Mke^{\frac{1}{k}}$ . For  $0 < k < 2$ , the equations for  $MSE_{min}$  and  $MSE_{max}$  merely get exchanged, but the illustration remains the same essentially. Because of the many-to-many mapping between  $L_2$  and  $L_p$ , the points in true operating region  $\mathcal{S}$  map to other  $L_p$ -norm values as well, and not just  $L_p = c_0$ . The  $\neg\mathcal{S} \cap \mathcal{S}^*$  region maps to  $L_p \neq c_0$ . The points  $A, B, C, D$  refer to the points  $A, B, C, D$  from Figure 2, except that here:  $\frac{MSE_{min}^{0.5}}{\sigma_G} = \frac{L_k}{\sqrt{N}\sigma_G} = 1.5$  and  $\theta_{max} = \frac{8}{1.5} = 5.\bar{3}$  (instead of 0.75 and 8 respectively).

Evaluation of the properties (such as the parametric equation, shape, existence of voids and discontinuities) of  $\mathcal{S}$  in the  $\{L_2, \rho_c\}$  space likewise as a function of the given gold standard for a fixed  $L_p$  norm ( $p \neq 2$ ) (cf. Figure 3) is a possible future research direction.

In summary, the operating regions in Figure 2 are constrained by the plots  $\rho_{c_{max}'}$  and  $\rho_{c_{min}'}$   $\Big|_{\theta \in [1, \theta_{max}(N)]}$  as per the Equation (20). While it is true that a given  $MkE$  (effectively, a given  $L_p$  norm) translates to a restricted range for  $MSE$  (cf. Equations (15) and (16)), these  $MSE$  extremities do not necessarily translate to  $\rho_c$  optimisation as dictated by Equation (20) (cf. Figure 3). Rather, it is  $\frac{MSE}{\sigma_{XY}}$  metric that needs to be optimised to find the optimised error distribution and sequence  $D_{optimised}$  optimising  $\rho_c$ , when given *any* constraint on  $D := (d_i)_1^N$  – e.g., a constant  $L_p$  norm. Investigation of the shape and properties of the span of the valid  $(L_p, \rho_c)$  pairs in the two dimensional  $\{L_p, \rho_c\}$  space (similar to Figure 1, but for  $p \neq 2$ ) is yet another possible future research direction.

We evaluate the conditions and formulation for these in the section next. by optimising the function  $\frac{MSE}{\sigma_{XY}}$  (cf. Equation (4)) and not just  $MSE$ , subject to the constraint: given  $L_p = \left(\sum_{i=1}^N |x_i - y_i|^p\right)^{\frac{1}{p}}$ .

## 7. $\rho_c$ optimisation, given $L_p$ ( $p = 2m, \forall m \in \mathbb{N}$ )

We generalise the Section 4 to any given  $L_p$  norm for every even  $p$ , beyond  $p = 2$ . The problem statement is, thus:

Given (1) a gold standard sequence,  $G := (g_i)_1^N$ , and (2) a fixed  $L_p, p = 2m, \forall m \in \mathbb{N}$ , find the set(/s) of error values  $E := (e_i)_1^N$  that achieve maximisation and minimisation of  $\rho_c$ .

For the prediction  $X := (x_i)_1^N$  and the gold standard sequence  $Y := (y_i)_1^N$  or  $G := (g_i)_1^N$ ,

$$\begin{aligned} \text{Maximise: } f(\{d_i\}_1^N) &= \frac{N \cdot \sigma_{XY}}{N \cdot MSE} = \frac{\sum_{i=1}^N y_{z_i}^2 + \sum_{i=1}^N d_i y_{z_i}}{\sum_{i=1}^N d_i^2}, \\ \text{subject to: } g(\{d_i\}_1^N) &= \sum_{i=1}^N |d_i|^k - N \cdot M k E = \sum_{i=1}^N d_i^k - N \cdot M k E = 0 \quad (\because k=2m, m \in \mathbb{N}). \end{aligned}$$

With  $f$  and  $g$  continuous and differentiable  $\forall d_i \in \mathbb{R}$ , the auxiliary Lagrange expression  $\mathcal{L}$  is:

$$\begin{aligned} \mathcal{L}(d_1, d_2, \dots, d_N, \lambda) &= f(d_1, d_2, \dots, d_N) - \lambda \cdot g(d_1, d_2, \dots, d_N), \\ \mathcal{L} &= \frac{\sigma_{XY}}{MSE} - \lambda \left( \sum_{i=1}^N d_i^k - N \cdot M k E \right). \end{aligned} \quad (21)$$

$$\therefore \nabla_{d_1, d_2, \dots, d_N, \lambda} \mathcal{L} = 0 \Leftrightarrow \begin{cases} \frac{\partial}{\partial d_i} \mathcal{L} = 0 \because \frac{\partial}{\partial d_i} \left( \frac{\sigma_{XY}}{MSE} \right) - \lambda k d_i^{k-1} = 0 \forall i \in \mathbb{N} : i \in [1, N]. \\ \frac{\partial}{\partial \lambda} \mathcal{L} = 0 \because \sum_{i=1}^N d_i^k - N \cdot M k E = 0. \end{cases} \quad (22)$$

$$\begin{aligned} \frac{\partial}{\partial d_i} \left( \frac{\sigma_{XY}}{MSE} \right) &= \frac{MSE \cdot \frac{\partial}{\partial d_i} \sigma_{XY} - \sigma_{XY} \cdot \frac{\partial}{\partial d_i} MSE}{MSE^2}, \\ \therefore 0 &= \frac{\partial}{\partial d_i} \mathcal{L} = \frac{MSE \cdot \frac{\partial}{\partial d_i} \sigma_{XY} - \sigma_{XY} \cdot \frac{\partial}{\partial d_i} MSE}{MSE^2} - \lambda k d_i^{k-1}, \\ \therefore \lambda k d_i^{k-1} &= \frac{MSE \cdot \frac{\partial}{\partial d_i} \sigma_{XY} - \sigma_{XY} \cdot \frac{\partial}{\partial d_i} MSE}{MSE^2}, \\ &= \frac{MSE \cdot \frac{\partial}{\partial d_i} \sum_{i=1}^N y_{z_i} d_i - \sigma_{XY} \cdot \frac{\partial}{\partial d_i} \sum_{i=1}^N d_j^2}{N \cdot MSE^2}, \\ \therefore d_i^k &= \frac{MSE \cdot y_{z_i} d_i - 2d_i^2(\sigma_G^2 + \sigma_{GD})}{\lambda k N MSE^2} \quad (\because \text{Equation (7)}), \end{aligned} \quad (23)$$

where:  $\sigma_{GD} = \frac{\sum_{i=1}^N y_{z_i} d_i}{N}$  : Covariance between  $G$  and  $D$ .

$$\begin{aligned} \therefore \sum_{i=1}^N \frac{d_i^k}{N} &= M k E = \sum_{i=1}^N \frac{MSE \cdot \frac{y_{z_i} d_i}{N} - 2 \frac{d_i^2}{N} (\sigma_G^2 + \sigma_{GD})}{\lambda \cdot k \cdot N \cdot MSE^2}, \\ \therefore M k E &= \frac{MSE \cdot \sigma_{GD} - 2 \cdot MSE \cdot (\sigma_G^2 + \sigma_{GD})}{\lambda \cdot k \cdot N \cdot MSE^2}, = \frac{-(2\sigma_G^2 + \sigma_{GD})}{\lambda \cdot k \cdot N \cdot MSE}, \\ \therefore \lambda \cdot k \cdot N \cdot MSE^2 &= \frac{-(2\sigma_G^2 + \sigma_{GD}) \cdot MSE}{M k E} \quad (= \text{denominator in Equation (23)}), \\ \therefore d_i^k &= -M k E \frac{MSE \cdot y_{z_i} d_i - 2d_i^2(\sigma_G^2 + \sigma_{GD})}{(2\sigma_G^2 + \sigma_{GD}) \cdot MSE}. \end{aligned}$$

$$\therefore d_i^k \cdot (2\sigma_G^2 + \sigma_{GD}) \cdot MSE = -MkE \cdot (MSE \cdot y_{z_i} d_i - 2d_i^2 \sigma_G^2 - 2d_i^2 \sigma_{GD}) \quad (24)$$

$$\therefore 2\sigma_G^2 \cdot \left( \frac{d_i^k}{MkE} - \frac{d_i^2}{MSE} \right) + \sigma_{GD} \cdot \left( \frac{d_i^k}{MkE} - 2\frac{d_i^2}{MSE} \right) + y_{z_i} d_i = 0. \quad (25)$$

Dividing Equation (24) by  $d_i$ , and expressing  $\sigma_{GD}$  and  $MSE$  in terms of  $d_i$ , we get a polynomial in  $d_i$ :

$$\begin{aligned} 0 &= 2\mathbf{d}_i^{k+1} \left( \sum_{\forall j} y_{z_j}^2 \right) + 2\mathbf{d}_i^{k-1} \left( \sum_{\forall j} y_{z_j} \right) \left( \sum_{j \neq i} d_j^2 \right) \\ &+ \mathbf{d}_i^{k+2} y_i + \mathbf{d}_i^k y_i \left( \sum_{j \neq i} d_j^2 \right) + \mathbf{d}_i^{k+1} \left( \sum_{j \neq i} y_{z_j} d_j \right) + \mathbf{d}_i^{k-1} \left( \sum_{j \neq i} y_{z_j} d_j \right) \left( \sum_{j \neq i} d_j^2 \right) \\ &+ N \cdot MkE \cdot \left( y_{z_i} \mathbf{d}_i^2 + y_{z_i} \sum_{j \neq i} d_j^2 - 2\mathbf{d}_i \sum_{\forall j} y_{z_j}^2 - 2\mathbf{d}_i^2 y_{z_i} - 2\mathbf{d}_i \sum_{j \neq i} y_{z_j} d_j \right) \end{aligned} \quad (26)$$

Solving Equation (26) for  $d_i$  in terms of  $y_{z_i}$ , i. e.,  $d_i = \zeta(y_{z_i})$ , one finds an optimal  $\{d_i\}_1^N$  maximising  $\rho_c$ . For example, substituting  $k = 2$  results in Equations (5) and (10) derived in Section 4 (cf. Appendix I).

Rewriting Equation (25) in terms of  $y_{z_i}$ , we get:

$$\begin{aligned} 0 &= \sum_{j=1}^N y_{z_j}^2 \left( \frac{d_i^{k-1}}{MkE} - \frac{d_i}{MSE} \right) + \sum_{j=1}^N y_{z_j} \cdot d_j \cdot \left( \frac{d_i^{k-1}}{MkE} - 2\frac{d_i}{MSE} \right) + y_{z_i} \\ &= \sum_{j=1}^N y_{z_j}^2 \left( d_i^{k-1} \cdot MSE - d_i \cdot MkE \right) + \sum_{j=1}^N y_{z_j} \cdot d_j \cdot \left( d_i^{k-1} \cdot MSE - 2d_i \cdot MkE \right) + y_{z_i} \cdot MSE \cdot MkE \\ &= y_{z_i}^2 \left( d_i^{k-1} \cdot MSE - d_i \cdot MkE \right) + y_{z_i} \cdot d_i \cdot \left( d_i^{k-1} \cdot MSE - 2d_i \cdot MkE \right) + y_{z_i} \cdot MSE \cdot MkE \\ &+ \sum_{j \neq i} y_{z_j}^2 \left( d_i^{k-1} \cdot MSE - d_i \cdot MkE \right) + \sum_{j \neq i} y_{z_j} \cdot d_j \cdot \left( d_i^{k-1} \cdot MSE - 2d_i \cdot MkE \right) \\ &= \mathbf{y}_{z_i}^2 + \mathbf{y}_{z_i} \left( d_i + \frac{MSE \cdot MkE - d_i^2 \cdot MkE}{d_i^{k-1} \cdot MSE - d_i \cdot MkE} \right) + \left[ \sum_{j \neq i} y_{z_j} \left( y_{z_j} + d_j \frac{d_i^{k-1} \cdot MSE - 2d_i \cdot MkE}{d_i^{k-1} \cdot MSE - d_i \cdot MkE} \right) \right] \end{aligned} \quad (27)$$

Solving quadratic Equation (27) would result in expression of  $y_{z_i}$  in terms of  $d_i$ , possibly free of  $y_{z_j}$ , for  $j \neq i$ . We note that this true optimisation formulation (cf. Equations (26) and (27)) is different than that we obtained in Section 5 (cf. Equation (20)), where only  $MSE$  was optimised instead of  $\frac{\sigma_{XY}}{MSE}$ .

## 8. $\rho_c$ optimisation, given the error-set

Different conditions on the error-set for  $\rho_c$  minimisation and maximisation in Section 4 establish the relevance of error values for  $\rho_c$  evaluation, for a given  $MSE$ . In this section, we prove that not only the values of the individual errors, but also their order directly impacts the  $\rho_c$  metric evaluation. To this end, we attempt to decouple the components of  $\rho_c$  that are dependent on merely the values of errors, from those directly impacted by the ‘sequence’/ordering of the errors. The problem statement is, thus:



Given (1) a gold standard time series,  $G := (g_i)_1^N$ , and (2) a fixed set of error values,  $E := (e_i)_1^N$  (thus a fixed MSE), find the distribution(s) or correspondence(s) of error values with respect to the gold standard that achieve(s) the highest possible  $\rho_c$ .

Let the prediction and the gold standard sequences be  $X := (x_i)_1^N$  and  $Y := (y_i)_1^N$ , not necessarily in that order. Note that, the sequence to variable correspondence does not affect  $\rho_c$  evaluation – since the  $\rho_c$  formulation is symmetric with respect to  $X$  and  $Y$ .

### 8.1 Formulation 1: Replacing $(x_i)$ with $(y_i + d_i)$

From Equation (4), we have:  $\rho_c = \left(1 + \frac{N \cdot MSE}{2 \sum_{i=1}^N (y_i - \mu_Y + d_i - \mu_D)(y_i - \mu_Y)}\right)^{-1}$ .

Note that  $\sum_{i=1}^N \mu_D (y_i - \mu_Y) = \mu_D \sum_{i=1}^N (y_i - \mu_Y) = \mu_D (N\mu_Y - N\mu_Y) = 0$ .

$$\begin{aligned} \therefore \rho_c &= \left(1 + \frac{N \cdot MSE}{2 \sum_{i=1}^N (y_i - \mu_Y)^2 + 2 \sum_{i=1}^N y_i d_i - 2 \sum_{i=1}^N \mu_Y d_i}\right)^{-1}, \\ &= \left(1 + \frac{N \cdot MSE}{2N\sigma_Y^2 + 2 \sum_{i=1}^N \mathbf{y}_i \mathbf{d}_i - 2N\mu_Y \mu_D}\right)^{-1}. \end{aligned}$$

$$\therefore \left(1 + \frac{a}{b}\right)^{-1} = \left(1 - \frac{a}{a+b}\right) \implies \rho_c = \left(1 - \frac{N \cdot MSE}{2N(\sigma_Y^2 - \mu_Y \mu_D) + 2 \sum_{i=1}^N \mathbf{y}_i \mathbf{d}_i + N \cdot MSE}\right). \quad (28)$$

Given a gold standard  $Y$  and  $\{d_i\}$ ,  $\rho_c$  maximisation necessitates  $\sum_{i=1}^N (\mathbf{y}_i) \mathbf{d}_i$  **maximisation**.

### 8.2 Formulation 2: Replacing $(y_i)$ with $(x_i - d_i)$

$$\text{Likewise (Cf. Appendix D), } \rho_c = \left(1 - \frac{N \cdot MSE}{2N(\sigma_X^2 + \mu_X \mu_D) - 2 \sum_{i=1}^N \mathbf{x}_i \mathbf{d}_i + N \cdot MSE}\right). \quad (29)$$

Given a gold standard  $X$  and  $\{d_i\}$ ,  $\rho_c$  maximisation necessitates  $\sum_{i=1}^N (\mathbf{x}_i) \mathbf{d}_i$  **minimisation**.

### 8.3 Paradoxical nature of the conditions on the error-set

The concluding remarks of Section 8.1 and Section 8.2 imply that we arrive at mutually contradictory requirements in terms of the rearrangement of values in the error-set. This is only an apparent paradox, since given a set of error values ( $E$ ) and a gold standard sequence ( $G$ ), two different candidate prediction sequences ( $P = G + E$  or  $P = G - E$ ) may be generated yielding a high  $\rho_c$ . When devising a loss function in terms of the predicted sequence itself, however, the requirements implied by both formulations converge to the same conditions. We discuss next this rediscovery of consistency, arising out of the prima facie mutually contradictory insights interestingly.

### 8.3.1 CONTRADICTORY REQUIREMENTS IN TERMS OF THE $\left(\sum_{i=1}^N \mathbf{g}_i \mathbf{e}_i\right)$ SUMMATION

Specifically, to maximise  $\rho_c$ :

- The formulation in the Section 8.1 requires *maximisation* of the  $\left(\sum_{i=1}^N \mathbf{g}_i \mathbf{e}_i\right)$  quantity.
- The formulation in the Section 8.2 requires *minimisation* of the  $\left(\sum_{i=1}^N \mathbf{g}_i \mathbf{e}_i\right)$  quantity.

### 8.3.2 CONTRADICTORY REQUIREMENTS IN TERMS OF THE ERROR-SET PERMUTATION

- Maximisation of  $\left(\sum_{i=1}^N \mathbf{g}_i \mathbf{e}_i\right)$  (as per Section 8.1) necessitates that the error values are in the *same* sorted order as of the gold standard values (cf. Appendix E).
- That is, a bigger  $e_i$  corresponds to a bigger  $g_i$ .
- Minimisation of  $\left(\sum_{i=1}^N \mathbf{g}_i \mathbf{e}_i\right)$  (as per Section 8.2) necessitates that the error values are in the *opposite* order as of the gold standard values (cf. Appendix E).
- That is, a smaller  $e_i$  corresponds to a bigger  $g_i$ .

In other words, taking into account both the magnitudes and the signs, the error values need to be sorted in the same order as of the elements of the time series, as dictated by the first (Section 8.1)  $\rho_c$  formulation. The second formulation (Section 8.2) dictates to the contrary; the errors need to be sorted in exactly the opposite order as of the sorted elements of the gold-standard time series. Thus, there exist two prediction sequences corresponding to an identical set of errors (with respect to the gold standard sequence), that maximise  $\rho_c$ .

### 8.3.3 CONSISTENT REQUIREMENTS IN TERMS OF THE $\left(\sum_{i=1}^N \mathbf{g}_i \mathbf{p}_i\right)$ SUMMATION

While there exist two distinct prediction sequences with an identical error-set (and thus an identical *MSE*), and despite the contradictory requirements in terms their permutations, we establish next that the conditions for the  $\rho_c$  maximisation in terms of the product summation  $\sum_{i=1}^N \mathbf{g}_i \mathbf{p}_i$  are consistent in both these formulations.

According to the first formulation (Section 8.1),

- $E = P - G$ , i. e.,  $(e_i)_1^N = (p_i)_1^N - (g_i)_1^N$ , and  $\left(\sum_{i=1}^N \mathbf{g}_i \mathbf{e}_i\right)$  needs to be maximised.
- That is,  $\left(\sum_{i=1}^N \mathbf{g}_i (\mathbf{p}_i - \mathbf{g}_i)\right)$  needs to be maximised, implying that  $\left(\sum_{i=1}^N \mathbf{g}_i (\mathbf{p}_i)\right)$  needs to be *maximised* – since  $\left(\sum_{i=1}^N \mathbf{g}_i^2\right)$  is constant for a given gold standard.

According to the second formulation (Section 8.2),

- $E = G - P$ , i. e.,  $(e_i)_1^N = (g_i)_1^N - (p_i)_1^N$ , and  $\left(\sum_{i=1}^N \mathbf{g}_i \mathbf{e}_i\right)$  needs to be minimised.
- That is,  $\left(\sum_{i=1}^N \mathbf{g}_i (\mathbf{g}_i - \mathbf{p}_i)\right)$  needs to be minimised, implying that  $\left(\sum_{i=1}^N \mathbf{g}_i (\mathbf{p}_i)\right)$  needs to be *maximised* – since  $\left(\sum_{i=1}^N \mathbf{g}_i^2\right)$  is constant for a given gold standard.

#### 8.4 Optimal $\rho_c$ formulation, given the error-set

Let  $\overset{1}{E} = (\overset{1}{e}_i)_1^N$  = the reordered  $P - G$  error sequence (cf. Section 8.1), and  $\overset{2}{E} = (\overset{2}{e}_i)_1^N$  = the reordered of ' $G - P$ ' error sequence (cf. Section 8.2) denote the two optimal error permutations corresponding to the sorted rearrangement of  $G := \bar{G} = (\bar{g}_i)_1^N$  for  $\rho_c$  maximisation. From Appendix G and section 8.3.3:

$$\begin{array}{l} \text{if for} \\ \text{then for} \end{array} \quad \begin{array}{ccccccc} \bar{G}, & \bar{g}_1 & \geq & \bar{g}_2 & \cdots & \geq & \bar{g}_N, \\ \overset{1}{E} : & \overset{1}{e}_1 & \geq & \overset{1}{e}_2 & \cdots & \geq & \overset{1}{e}_N, \end{array} \quad (30)$$

$$\text{and for} \quad \overset{2}{E} : \quad \overset{2}{e}_1 \leq \overset{2}{e}_2 \leq \cdots \leq \overset{2}{e}_N, \quad (31)$$

$$\begin{array}{l} \text{i. e.,} \\ \therefore \end{array} \quad \begin{array}{ccccccc} \overset{2}{E} : & \overset{2}{e}_N & \geq & \overset{2}{e}_{N-1} & \cdots & \geq & \overset{2}{e}_1, \\ & \overset{2}{e}_j & = & \overset{1}{e}_{N+1-j} & & \forall j \in \mathbb{N} : j \in [1, N]. \end{array} \quad (32)$$

$$\text{Thus, } \rho_{c_{max1}} = \left( 1 - \frac{N(MSE)}{2N\sigma_G^2 + 2\sum_{i=1}^N \bar{g}_i \overset{1}{e}_i - 2N\mu_G\mu_E + N \cdot MSE} \right) \quad \because \text{Equations (28) and (30),} \quad (33)$$

$$\rho_{c_{max2}} = \left( 1 - \frac{N(MSE)}{2N\sigma_G^2 - 2\sum_{i=1}^N \bar{g}_i \overset{2}{e}_i + 2N\mu_G\mu_E + N \cdot MSE} \right) \quad \because \text{Equations (29) and (30),} \quad (34)$$

$$\rho_{c_{min1}} = \left( 1 - \frac{N(MSE)}{2N\sigma_G^2 + 2\sum_{i=1}^N \bar{g}_i \overset{2}{e}_i - 2N\mu_G\mu_E + N \cdot MSE} \right) \quad \because \text{Equations (28) and (31),} \quad (35)$$

$$\rho_{c_{min2}} = \left( 1 - \frac{N(MSE)}{2N\sigma_G^2 - 2\sum_{i=1}^N \bar{g}_i \overset{1}{e}_i + 2N\mu_G\mu_E + N \cdot MSE} \right) \quad \because \text{Equations (29) and (31).} \quad (36)$$

**Remark 7** From the equations above, following observations can be made:

- The denominators in Equations (33) and (34) are strictly non-negative (cf. Chebyshev's sum inequality in Appendix G), and are strictly  $\leq N \cdot MSE$ . Which implies:  $0 \leq \rho_{c_{max1}}, \rho_{c_{max2}} \leq 1$ .
- In other words, there exists a permutation of every possible error-set that results in a non-negatively correlated prediction sequence, irrespective of the definition or formulation of the error sequence used (i. e., whether  $P - G$  or  $G - P$ ), and irrespective of the MSE the error sequence amounts to.
- $\rho_{c_{max1}}, \rho_{c_{max2}} \rightarrow 0$  only when  $MSE \rightarrow \infty$ . Both these inferences are consistent with Figure 1.
- As per Chebyshev's sum inequality (cf. Appendix G) and from Equations (30) and (31):

$$\begin{aligned} & 2\sum_{i=1}^N \bar{g}_i \overset{2}{e}_i - 2N\mu_G\mu_E \leq 0 \quad \text{and} \quad -2\sum_{i=1}^N \bar{g}_i \overset{1}{e}_i + 2N\mu_G\mu_E \leq 0 \\ \implies & \rho_{c_{min1}}, \rho_{c_{min2}} \leq 0 \quad \text{for a smaller } \frac{\sigma_G^2}{MSE} \quad \because \text{Equations (35) and (36).} \end{aligned}$$

This observation is consistent with Figure 1, where:  $-1 \leq \rho_{c_{min}} \leq 0$  for  $\frac{MSE}{\sigma_G^2} \geq 1$ .

- A generalisation, or determining conclusively  $\rho_{c_{max1}} \stackrel{\geq}{\leq} \rho_{c_{max2}}$  is not possible (cf. Appendix H).

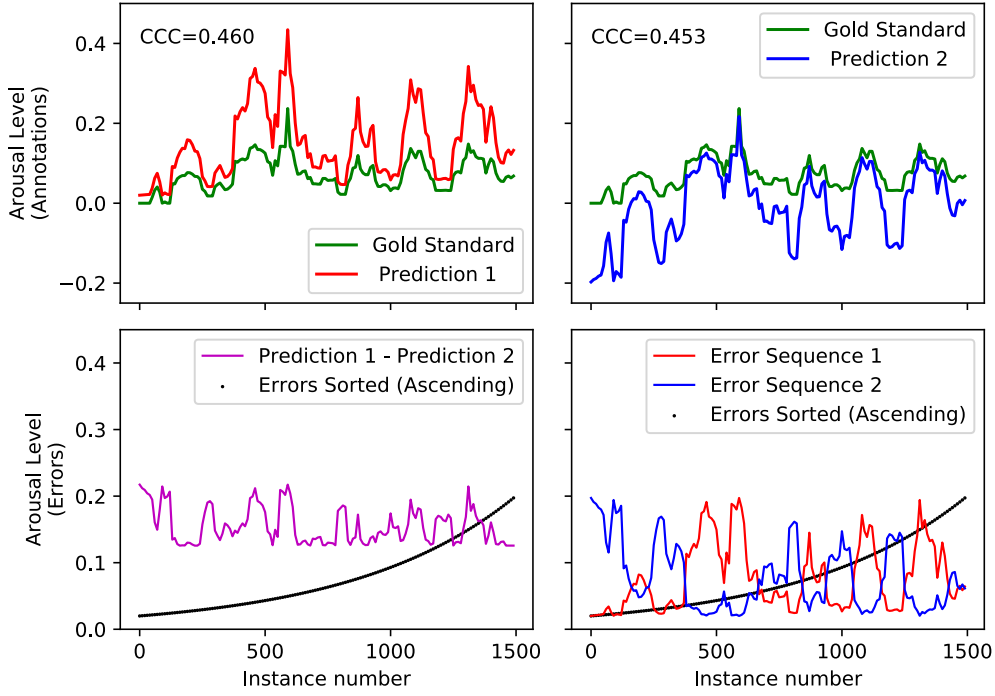


Figure 4: A reproducible illustration of an identical error-set resulting in different performance in terms of  $\rho_c$  through reordering. The gold standard sequence used (in green) is the *Train\_04* arousal annotation from the *SEWA/AVEC'17* database (Kossaifi et al., 2019; Ringeval et al., 2017). The two error sequences, the sorted error sequence, and the difference between the two predictions are in the bottom row of the plots. The errors are ordered such that they maximise  $\rho_c$  (as per Equations (30) and (31)), shown in red and blue respectively in the top row. The resulting two  $\rho_c$  are not drastically different in the example above. Because  $MSE$  is large enough in this particular case, with a different permutation, a close-to-zero or a negative  $\rho_c$  can be obtained as well (cf. [https://github.com/vedhasua/mse\\_ccc\\_corollary/](https://github.com/vedhasua/mse_ccc_corollary/)).

## 8.5 Dataset example with illustrations

Figure 4 illustrates how the two different optimal permutations of the same error-set, as per the  $\rho_c$  formulations from Equations (33) and (34) translate to two different prediction sequences (i. e.,  $P = G + E$  and  $P = G - E$ ), and thus two different  $\rho_{c_{max}}$ . The database we used to generate Figure 4 is the gold standard sequence of *Train\_04* arousal levels from the *SEWA/AVEC'17* database (Kossaifi et al., 2019; Ringeval et al., 2017). The database has recently gained a lot of popularity in the affective computing community, as it was used in all of the recent Audio/Visual Emotion Challenges (AVEC) (Ringeval et al., 2017, 2018a,b), where  $\rho_c$  was the decision criteria for recognising the winning submission. Note that the results presented are fully reproducible with an easy-to-use scripts we have made available at [https://github.com/vedhasua/mse\\_ccc\\_corollary/](https://github.com/vedhasua/mse_ccc_corollary/) that use a publicly available *SEWA/AVEC'17* dataset, or by using *any* ordinal data that one can own or can generate.

The green line-plot represents the gold standard sequence always. Different error sequences give rise to blue, red and black line-plots in the bottom right subplot, of which the black one represents the sorted error-set. ‘Prediction 1’ and ‘Prediction 2’ correspond to  $\rho_{c_{max_1}}$  and  $\rho_{c_{max_2}}$  (cf. Equations (33) and (34)).

For the sake of simplicity and clarity in the illustration, we chose the error values to be strictly positive, where the minimum of the errors is close to zero. Observing the locations of the tiniest of the errors, we note that the first prediction sequence attempts to closely follow the lower values in the gold standard, while the latter closely follows the bigger values, consistent to the discussion in Section 8.3.

We also note that the two prediction sequences are quite similar in shape to one another, but are far from being identical. The two are non-linearly stretched in the vertical direction, i. e., owing to the reordering of different errors. The second row of plots provides a better insight into this vertical stretching. Comparing the magenta and the green-coloured plot, it can be seen that the difference between the two prediction sequences is the highest at the extremities of the gold standard. This is expected, since the smallest error is associated with either the smallest (Equation (30)) or the biggest (Equation (31)) sample.

## 9. Additional loss functions and the interpretations

Equation (4) dictates the need for minimisation the  $L_p$  norm of the error values, i. e.,  $MSE = N \cdot \sum_{j=1}^N (g_j - p_j)^2$ , while simultaneous maximisation of the DotProduct( $G, P$ ) =  $DP = \sum_{i=1}^N g_i p_i$  (aka Hadamard product) to achieve  $\rho_c$  maximisation. A family of loss functions, such as the following, can be easily designed.

$$f(g_i, p_i) = \frac{\sum_{j=1}^N (g_j - p_j)^2}{\sum_{j=1}^N g_j p_j}, \quad (37)$$

$$\text{more generally, } f(g_i, p_i) = \left| \frac{\sum_{j=1}^N (g_j - p_j)^2}{\sum_{j=1}^N g_j p_j} \right|^\gamma \quad \text{where } \gamma > 0, \quad (38)$$

$$\text{even more generally, } f(g_i, p_i) = \left| \frac{\sum_{j=1}^N \varepsilon_j (g_j - p_j)^2}{\sum_{j=1}^N \alpha_i (g_j p_j)^{2\beta_j + 1}} \right|^\gamma \quad \text{where } \alpha_j, \beta_j, \varepsilon_j, \gamma > 0, \beta_j \in \mathbb{N}. \quad (39)$$

$$\text{Or } f(g_i, p_i) = \sum_{j=1}^N (g_j - p_j)^2 - \alpha \sum_{j=1}^N g_j p_j, \quad \text{where } \alpha > 0, \quad (40)$$

$$\text{more generally, } f(g_i, p_i) = \left| \sum_{j=1}^N (g_j - p_j)^2 - \alpha \sum_{j=1}^N (g_j p_j)^{2\beta + 1} \right|^\gamma \quad \text{where } \alpha, \beta, \gamma > 0, \beta \in \mathbb{N}, \quad (41)$$

$$\text{even more generally, } f(g_i, p_i) = \left| \sum_{j=1}^N \varepsilon_j (g_j - p_j)^2 - \sum_{j=1}^N \alpha_i (g_j p_j)^{2\beta_j + 1} \right|^\gamma \quad \text{where } \alpha_j, \beta_j, \varepsilon_j, \gamma > 0, \beta_j \in \mathbb{N}. \quad (42)$$

A loss function, attempting to maximise  $\sum_{i=1}^N g_i p_i$ , i. e., the dot product between the predictions and the gold standard, makes sense intuitively as well. We essentially dictate the model to raise the prediction values as large as possible when dealing with large values in the gold standard sequence, and diminish the predictions to as small as possible corresponding to the smaller values in the gold standard sequence. The  $MSE$  metric as a sub-component of the derived loss function, too, attempts to achieve this. However, the inner workings differ slightly. The  $MSE$  component drives the weights of the model to readjust by the amount that is proportional to the error seen, through back-propagation. The dot product readjusts the weights by an amount that is proportional to the gold standard itself. From another perspective, we effectively ‘weigh’ the individual errors by the corresponding desired outputs.

## 9.1 Role of the constants $\alpha, \beta, \alpha_j, \beta_j, \varepsilon_j, \gamma$ in Equations (37) to (42)

While it is possible to use the deviation from the maximally achievable  $\rho_c$  (i. e.,  $1 - \rho_c$ ) as the loss function (Trigeorgis et al., 2016; Schmitt et al., 2019; Pandit et al., 2020), the joint variability of the prediction and the gold standard can also be simultaneously improved using  $\frac{MSE}{\sigma_{XY}}$  as the loss function directly (cf. Equation (4)), i. e., using Equation (37) as the loss function.  $\rho_c$  maximisation could then be expected through simultaneous  $MSE$  minimisation with  $\sigma_{XY}$  maximisation. However, one drawback of  $\frac{MSE}{\sigma_{XY}}$  as the loss function has been witnessed (Pandit et al., 2019); i. e., the neural network may ‘cheat’ by simply making  $\sigma_{XY}$  more and more negative, without attempting  $MSE$  minimisation. To avoid this, one can alternately use  $\left|\frac{MSE}{\sigma_{XY}}\right|^\gamma, \gamma > 0$ , i. e., Equation (38) as the loss function. While with  $\left|\frac{MSE}{\sigma_{XY}}\right|^\gamma$  as the objective function,  $\sigma_{XY}$  itself is still not guaranteed to be non-negative, the network now needs to maximise  $|\sigma_{XY}|$  (instead of minimising  $\sigma_{XY}$ ), while simultaneously minimising  $MSE$ . In other words, the key difference between the two functions is that, there is no lower bound for  $\frac{MSE}{\sigma_{XY}}$ . Thus, the ability of the network to ‘cheat’ gets rather restricted when using  $\left|\frac{MSE}{\sigma_{XY}}\right|^\gamma$ , since a highly negative  $\sigma_{XY}$  (i. e., a highly negative correlation) can only be obtained with high magnitude of errors, effectively resulting in a high  $MSE$ , thus a higher loss. This loss function too has been also proven to be successful in practice (Pandit et al., 2019).

Maximisation of  $\rho_c$  may also be encouraged by using a difference function such as the one in Equation (40) as the loss function, where  $\alpha$  denotes relative importance assigned to maximisation of  $\sigma_{XY}$  compared to minimisation of  $MSE$ . The dot product  $g_j p_j$  can be raised to an odd integer exponent  $2\beta + 1$  to retard or to expedite  $\sigma_{XY}$  minimisation process (cf. Equation (41)). Finally, the individual sample-level loss components can be emphasised using scalars  $\alpha_j, \beta_j, \varepsilon_j$  (cf. Equations (39) and (42)).

## 10. Concluding remarks

We derive the missing, yet fundamentally crucial many-to-many mapping existing between  $\rho_c$  and  $MSE$  – both arguably the most popular utility functions in use today. We discover the conditions necessary achieving the minimum and the maximum possible  $\rho_c$  at any given  $MSE$ , and likewise, for any given fixed  $L_p$  norm for any real-valued  $p$  greater than 0, through  $MSE$  optimisation. As the research community has often witnessed; while the two processes – namely the error  $L_p$  norm minimisation and the  $\rho_c$  maximisation – are elusively directed at the same goal, we conclusively prove that the two are neither necessarily identical, nor necessarily convergent – except at the very extremity, where the ideal set of zero-valued errors translates to a perfect identity relationship, i. e.,  $\rho_c = 1$ . In other words, we prove mathematically the reasons for the witnessed inconsistency; the observation often reported in the literature lately (Trigeorgis et al., 2016; Pandit et al., 2019; Atmaja and Akagi, 2020). We generalise the  $\rho_c$  optimisation strategy to any given error- $L_p$  norm, for any  $p$  that is even and not necessarily  $p = 2$ .

While we establish that not just  $L_k$ -norm value, but rather the *distribution* of the errors making  $L_k$  dictates the  $\rho_c$  metric performance, we prove further that even with a full knowledge of the set of error values (i. e., the error distribution), the  $\rho_c$  metric still can not be conclusively computed. The order (i. e., the correspondence of the error values with respect to the ground truth) also governs  $\rho_c$  metric. We establish the conditions for which  $\rho_c$  is maximised and minimised when given a fixed set of errors. There exist two different notions of what the ‘error’ actually means (i. e., whether the prediction minus the gold standard, or the other way around), we derive the  $\rho_c$  optimisation formulations for both these cases.

Keeping the deep learning models in perspective – that are capable of mapping even complex and non-linear input-to-output relationships – we propose a family of new loss functions, some of which have been tested and have been proven to work. With these loss functions, the models can be aimed to maximise  $\rho_c$ , with simultaneous minimisation of the errors and maximisation of the joint variability of the prediction with respect to the desired output. The proposed loss functions consist of two components. First component is the classical loss function  $MSE$  that reduces the difference between the prediction and the gold standard by an amount that is proportional to the error itself. Our newly introduced dot product or covariance-based component tunes the parameters of the model by an amount that is proportional to the value of the gold standard itself, through backpropagation. Through the rigorous derivation of the formula for the many-to-many mapping that exists between  $MSE$  and  $\rho_c$ , we also propose a rather more elegant loss function, which is simply the positive power of the absolute value of the ratio of  $MSE$  to  $\sigma_{XY}$ , i. e.,  $\left|\frac{MSE}{\sigma_{XY}}\right|^\gamma, \gamma > 0$ .

While we have derived the condition for  $\rho_c$  optimisation for a given  $L_p$  (cf. Equation (26)), the investigation of properties of span of  $\{L_p, \rho_c\}$  in the  $(L_p, \rho_c)$  and in the  $(L_2, \rho_c)$  space ( $p \neq 2$ ) remains an unsolved problem; a possible future research direction.

## Appendix A. Proof of Theorem 3

**Proof** To minimise  $\rho_c$ , according to Equations (4), (6) and (7), we need to

$$\text{maximise: } f(\{d_i\}) = -N\sigma_{XY} = -\sum_{i=1}^N y_{z_i}^2 - \sum_{i=1}^N d_i y_{z_i}, \quad \text{subject to: } g(\{d_i\}) = N \cdot MSE - \sum_{i=1}^N d_i^2 = 0.$$

Auxiliary Lagrange function  $\mathcal{L}(d_1, d_2, \dots, d_N, \lambda) = f(d_1, d_2, \dots, d_N) - \lambda \cdot g(d_1, d_2, \dots, d_N)$  is given by:

$$\begin{aligned} \mathcal{L} &= -\sum_{i=1}^N y_{z_i}^2 - \sum_{i=1}^N d_i y_{z_i} - \lambda \left( N \cdot MSE - \sum_{i=1}^N d_i^2 \right). \\ \therefore \nabla_{d_1, d_2, \dots, d_N, \lambda} \mathcal{L} = 0 &\Leftrightarrow \begin{cases} -y_{z_i} + 2\lambda d_i = 0 & \forall i \in \mathbb{N} : i \in [1, N], \\ N \cdot MSE - \sum_{i=1}^N d_i^2 = 0. \end{cases} \end{aligned} \quad (43)$$

$$\therefore d_i = \mp \sqrt{\frac{N \cdot MSE}{\sum_{j=1}^N y_{z_j}^2}} \cdot y_{z_j} = \mp \sqrt{\frac{MSE}{\sigma_G^2}} \cdot y_{z_j} \quad \because \text{Eqs. (8) and (43) are identical} \implies \text{Eq. (9)}. \quad (44)$$

$N\sigma_{XY}$  is minimised when  $d_i$  and  $y_{z_j}$  have opposite signs, and when

$$d_i = -\left| \sqrt{\frac{N \cdot MSE}{\sum_{j=1}^N y_{z_j}^2}} \right| \cdot y_{z_j} = -\left| \sqrt{\frac{MSE}{\sigma_G^2}} \right| \cdot y_{z_j} \quad \because \text{Equations (7) and (44)}.$$

$$\therefore \sigma_{XY \min} = \frac{1}{N} \left( \sum_{i=1}^N y_{z_i}^2 \left( 1 - \sqrt{\frac{MSE}{\sigma_G^2}} \right) \right) = \sigma_G^2 - \sqrt{\sigma_G^2 \cdot MSE} \quad \because \text{Equation (7)}.$$

$$\therefore \rho_{c \min} = \frac{2 \cdot \left( 1 - \sqrt{\frac{MSE}{\sigma_G^2}} \right)}{\frac{MSE}{\sigma_G^2} + 2 \left( 1 - \sqrt{\frac{MSE}{\sigma_G^2}} \right)} \implies \rho_{c \min} = \frac{2 \left( 1 - \sqrt{\frac{MSE}{\sigma_G^2}} \right)}{1 + \left( 1 - \sqrt{\frac{MSE}{\sigma_G^2}} \right)^2}.$$

■

## Appendix B. Proof of Equation (16)

**Proof** Hölder's inequality (cf. Appendix F) leads to the following famous identity for  $0 < r < p$ :

$$\begin{aligned}
 L_p &\leq L_r && \leq N^{\frac{p-r}{pr}} L_p. \\
 \therefore L_2 &\leq L_k && \leq N^{\frac{2-k}{2k}} \cdot L_2, \\
 \Rightarrow MSE^{\frac{1}{2}} &\leq N^{(\frac{1}{k}-\frac{1}{2})} \cdot M_k E^{\frac{1}{k}} && \leq N^{\frac{2-k}{2k}} \cdot MSE^{\frac{1}{2}}, \\
 \text{i. e., } M_k E^{\frac{1}{k}} &\leq MSE^{\frac{1}{2}} && \leq N^{\frac{2-k}{2k}} \cdot M_k E^{\frac{1}{k}}.
 \end{aligned}$$

■

Appendix C. Figure 2-equivalent for  $k < 2$  (e. g., for a given MAE, i. e., for  $k = 1$ )

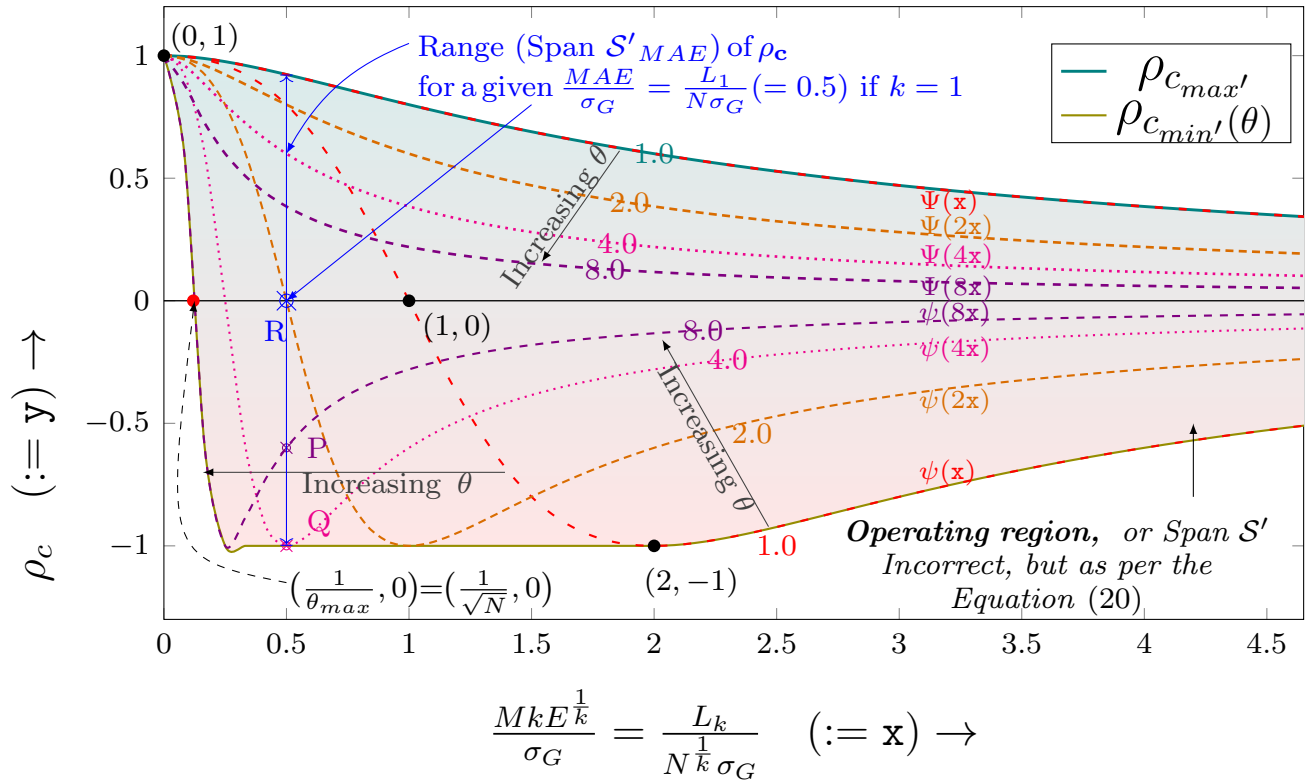


Figure 5: Range of  $\rho_c$  as per Equation (20), for a given MAE with respect to the gold standard consisting of  $N$  samples, standard deviation =  $\sigma_G^2$ ,  $1 \leq \theta \leq \sqrt{N}$ . Note the increase in the operating region  $\mathcal{S}'$  with a negative  $\rho_c$  due to the allowed variation in  $\rho_{c_{min}'} = \psi(\theta \cdot \mathbf{x})$  with increasing  $\theta$ . While each point in  $\mathcal{S}'$  maps to a unique  $\{MAE, \rho_c\}$  pair, each maps to infinitely many MSE values – except those on the  $\rho_{c_{max}'}$   $\rho_{c_{min}'}$  curves which map to only one possible MSE. Similar to Figure 1,  $MAE_1 \leq MAE_2$  does not always translate to  $\rho_{c_1} \leq \rho_{c_2}$ . For the sake of completeness, we note further that the true  $\rho_{c_{max}}$  and consequently, the true span  $\mathcal{S}$  is less than the one shown above (cf. Section 6). Note that the x-coordinate is  $\frac{L_K}{N^{\frac{1}{k}} \sigma_G}$  and consequently, the observations are true for any  $0 < k \leq 2$ , not necessarily for  $k = 1$  alone.



## Appendix D. Formulation 2: Replacing $(y_i)$ with $(x_i - d_i)$

From Equation (4), we have:  $\rho_{\mathbf{c}} = \left(1 + \frac{N \cdot MSE}{2 \sum_{i=1}^N (x_i - \mu_X)(x_i - \mu_X - d_i + \mu_D)}\right)^{-1}$ .

Note that  $\sum_{i=1}^N \mu_D(x_i - \mu_X) = \mu_D \sum_{i=1}^N (X_i - \mu_X) = \mu_D(N\mu_X - N\mu_X) = 0$ .

$$\begin{aligned} \therefore \rho_{\mathbf{c}} &= \left(1 + \frac{N \cdot MSE}{2 \sum_{i=1}^N (x_i - \mu_X)^2 - 2 \sum_{i=1}^N x_i d_i + 2 \sum_{i=1}^N \mu_X d_i}\right)^{-1}, \\ &= \left(1 + \frac{N \cdot MSE}{2N\sigma_X^2 - 2 \sum_{i=1}^N \mathbf{x}_i \mathbf{d}_i + 2N\mu_X \mu_D}\right)^{-1}. \\ \because \left(1 + \frac{a}{b}\right)^{-1} &= \left(1 - \frac{a}{a+b}\right) \implies \rho_{\mathbf{c}} = \left(1 - \frac{N \cdot MSE}{2N(\sigma_X^2 + \mu_X \mu_D) - 2 \sum_{i=1}^N \mathbf{x}_i \mathbf{d}_i + N \cdot MSE}\right). \end{aligned}$$

## Appendix E. The Rearrangement Inequality

The rearrangement inequality is a theorem concerning the rearrangements of two sets, to maximise and minimise the sum of element-wise products (Hardy et al., 1988).

Denoting the two sets  $(a) = \{a_1, a_2, \dots, a_n\}$  and  $(b) = \{b_1, b_2, \dots, b_n\}$ , let  $(\bar{a})$  and  $(\bar{b})$  be permutations of  $(a)$  and  $(b)$  sorted respectively, such that

$$\begin{array}{ccccccc} \bar{a}_1 & & \leq \bar{a}_2 & & \leq \dots & & \leq \bar{a}_n, \\ \text{and } \bar{b}_1 & & \leq \bar{b}_2 & & \leq \dots & & \leq \bar{b}_n. \end{array}$$

The rearrangement inequality states that

$$\sum_{j=1}^n \bar{a}_j \bar{b}_{n+1-j} \leq \sum_{j=1}^n a_j b_j \leq \sum_{j=1}^n \bar{a}_j \bar{b}_j.$$

More explicitly,

$$\begin{aligned} \bar{a}_n \bar{b}_1 + \dots + \bar{a}_1 \bar{b}_n &\leq \bar{a}_{\sigma(1)} \bar{b}_1 + \dots + \bar{a}_{\sigma(n)} \bar{b}_n \leq \bar{a}_1 \bar{b}_1 + \dots + \bar{a}_n \bar{b}_n, \\ &\text{for every permutation } \{\bar{a}_{\sigma(1)}, \bar{a}_{\sigma(2)}, \dots, \bar{a}_{\sigma(n)}\} \text{ of } \{\bar{a}_1, \dots, \bar{a}_n\}. \end{aligned}$$

For the unsorted ordered sets  $(a)$  and  $(b)$ , the two sets are said to be ‘similarly ordered’ or ‘monotonic in the same sense’ if  $(a_\mu - a_\nu)(b_\mu - b_\nu) \geq 0$  for all  $\mu, \nu$ , and ‘oppositely ordered’ or ‘monotonic in the opposite sense’ if the inequality is always reversed. With this notion of ‘similar’ and ‘opposite’ ordering, the maximum summation corresponds to the similar ordering of  $(a)$  and  $(b)$ . The minimum corresponds to the opposite ordering of  $(a)$  and  $(b)$ .

## Appendix F. Relationship between p-norms

According to Hölder's inequality,

$$\sum_{i=1}^n |a_i| |b_i| \leq \left( \sum_{i=1}^n |a_i|^t \right)^{\frac{1}{t}} \left( \sum_{i=1}^n |b_i|^{\frac{t}{t-1}} \right)^{1-\frac{1}{t}}.$$

Let  $|a_i| = |x_i|^r$ ,  $|b_i| = 1$  and  $t = p/r > 1$ .

$$\begin{aligned} \sum_{i=1}^n |x_i|^r &\leq \left( \sum_{i=1}^n (|x_i|^r)^{\frac{p}{r}} \right)^{\frac{r}{p}} \left( \sum_{i=1}^n 1^{\frac{p}{p-r}} \right)^{1-\frac{r}{p}} = \left( \sum_{i=1}^n |x_i|^p \right)^{\frac{r}{p}} n^{1-\frac{r}{p}}. \\ \therefore \|x\|_r &= \left( \sum_{i=1}^n |x_i|^r \right)^{\frac{1}{r}} \leq \left( \left( \sum_{i=1}^n |x_i|^p \right)^{\frac{r}{p}} n^{1-\frac{r}{p}} \right)^{\frac{1}{r}} = \left( \sum_{i=1}^n |x_i|^p \right)^{\frac{1}{p}} n^{\frac{1}{r}-\frac{1}{p}} = n^{1/r-1/p} \|x\|_p. \\ \text{Also, when } r < p, \quad &\|x\|_p \leq \|x\|_r. \\ \therefore \quad &\|x\|_p \leq \|x\|_r \leq n^{1/r-1/p} \|x\|_p. \end{aligned}$$

## Appendix G. Chebyshev's Sum Inequality

The Chebyshev's sum inequality (Hardy et al., 1988) states that

$$\begin{aligned} \text{if } a_1 \geq a_2 \geq \dots \geq a_n \quad \text{and} \quad b_1 \geq b_2 \geq \dots \geq b_n, \\ \text{then} \quad \frac{1}{n} \sum_{k=1}^n a_k \cdot b_k &\geq \left( \frac{1}{n} \sum_{k=1}^n a_k \right) \left( \frac{1}{n} \sum_{k=1}^n b_k \right), \\ \text{and if } a_1 \leq a_2 \leq \dots \leq a_n \quad \text{and} \quad b_1 \geq b_2 \geq \dots \geq b_n, \\ \text{then} \quad \frac{1}{n} \sum_{k=1}^n a_k b_k &\leq \left( \frac{1}{n} \sum_{k=1}^n a_k \right) \left( \frac{1}{n} \sum_{k=1}^n b_k \right). \end{aligned}$$

## Appendix H. Comparison between $\rho_{c_{max_1}}$ AND $\rho_{c_{max_2}}$

$$\begin{aligned} \text{Suppose} \quad \rho_{c_{max_1}} &\geq \rho_{c_{max_2}}, \\ \text{true if } 2 \sum_{i=1}^N \bar{g}_i^1 e_i - 2N\mu_G \mu_E &\geq -2 \sum_{i=1}^N \bar{g}_i^2 e_i + 2N\mu_G \mu_E, \\ \text{true if } \sum_{i=1}^N \bar{g}_i^1 e_i + \sum_{i=1}^N \bar{g}_i^2 e_i &\geq 2N\mu_G \mu_E, \\ \text{true if } \frac{1}{N} \sum_{i=1}^N \bar{g}_i^1 e_i + \frac{1}{N} \sum_{i=1}^N \bar{g}_i^2 e_i &\geq \left( \frac{1}{N} \sum_{k=1}^N \bar{g}_i \right) \left( \frac{1}{N} \sum_{k=1}^N (e_i^1 + e_i^2) \right), \\ \text{true if } \frac{1}{N} \sum_{i=1}^N \bar{g}_i (e_i^1 + e_{N-i+1}^1) &\geq \left( \frac{1}{N} \sum_{k=1}^N \bar{g}_i \right) \left( \frac{1}{N} \sum_{k=1}^N (e_i^1 + e_{N-i+1}^1) \right). \end{aligned} \quad (45)$$

We note that  $\frac{1}{N} \sum_{i=1}^N \bar{g}_i e_i \geq \left( \frac{1}{N} \sum_{k=1}^N \bar{g}_i \right) \left( \frac{1}{N} \sum_{k=1}^N e_i \right)$ , while  $\left( \frac{1}{N} \sum_{k=1}^N \bar{g}_i \right) \cdot \left( \frac{1}{N} \sum_{k=1}^N e_i^2 \right) \geq \frac{1}{N} \sum_{i=1}^N \bar{g}_i e_i^2$  according to the Chebyshev's sum inequality (cf. Appendix G). Also,  $\left( e_i + e_{N-i+1} \right)$  is symmetric with respect to  $i = \frac{N+1}{2}$  (cf. Equation (32)).

Because the sequence  $(e_i + e_{N-i+1})$  features both the similarly ordered and the oppositely ordered error components, no guarantees can be made in terms of veracity of Equation (45) using any of the two equalities we have used so far, i. e., the Chebyshev's sum inequality (Appendix G) and the rearrangement inequality (Appendix E). One needs to compute both the sides of the Equation (45) to determine which permutation of the errors results in the prediction with the higher  $\rho_c$ .

## Appendix I. Consistency checks / validations of the formulations

In this section, we cross-check the derived formulations, whether they are consistent with the formulations derived elsewhere independently for  $k = 2$ .

**Equation (25):**

$$\therefore 0 = 2\sigma_G^2 \cdot (0) + \frac{\sum_{j=1}^N \mathbf{y}_{z_j} d_j}{N} \cdot \left( \frac{-d_i^2}{\mathbf{MSE}} \right) + \mathbf{y}_{z_i} d_i \quad \therefore \text{Equation (25) and } MKE = MSE \text{ if } k = 2.$$

$$\therefore \mathbf{y}_{z_i} d_i = \frac{d_i^2}{N \cdot \mathbf{MSE}} \sum_{j=1}^N \mathbf{y}_{z_j} d_j \implies \mathbf{y}_{z_i} = d_i \frac{\sigma_{GD}}{\mathbf{MSE}} \quad \forall i \in [1, N]. \quad (46)$$

$$\therefore \sum_{i=1}^N \mathbf{y}_{z_i}^2 = \sum_{i=1}^N \mathbf{y}_{z_i} d_i \left( \frac{\sigma_{GD}}{\mathbf{MSE}} \right) \implies N\sigma_G^2 = N \frac{\sigma_{GD}^2}{\mathbf{MSE}} \quad \therefore \sigma_{GD} = \pm \sqrt{\frac{\mathbf{MSE}}{\sigma_G^2}}. \quad (47)$$

Substituting  $\sigma_{GD}$  in Equation (46) for a positive covariance:

$$\therefore d_i = \left| \sqrt{\frac{\mathbf{MSE}}{\sigma_G^2}} \right| \cdot y_{z_i} \quad \forall i \in [1, N], \quad (\text{identical to Equation (5) from Section 4}).$$

Likewise, for  $\rho_c$  minimisation, use  $f = -\frac{\sigma_{XY}}{\mathbf{MSE}}$  and  $g = N \cdot MKE - \sum_{i=1}^N d_i^k$  results in Equation (21). This leads to identical constraints given by Equation (22), leading to the same solution Equation (25), and thus, Equation (47). However, in this case, the ratio  $\frac{y_{z_i}}{d_i}$  needs to be negative for the solution to correspond to  $\rho_{c_{min}}$ , resulting in Equation (10) from Section 4.

**Equations (15) and (16):**

Substituting  $k = 2$  in Equations (15) and (16)), gives us  $\theta_{max} = 1$ . Consequently, Figure 2 gets transformed into Figure 1, consistent with Section 4 findings.

## Appendix J. Resources in the interest of reproducibility

The findings and the results presented are fully reproducible with an easy-to-use scripts and data made available at [https://github.com/vedhasua/mse\\_ccc\\_corollary/](https://github.com/vedhasua/mse_ccc_corollary/). The provided script uses a sample sequence from a publicly available *SEWA/AVEC'17* dataset. One may also use any other ordinal dataset as an input to the provided script, and witness the results consistent to the findings presented in the manuscript.

## References

- Greg Atkinson and Alan M Nevill. Statistical methods for assessing measurement error (reliability) in variables relevant to sports medicine. *Sports medicine*, 26(4):217–238, 1998.
- Bagus Tris Atmaja and Masato Akagi. Evaluation of error and correlation-based loss functions for multitask learning dimensional speech emotion recognition. *arXiv preprint arXiv:2003.10724*, 2020.
- Mousumi Banerjee, Michelle Capozzoli, Laura McSweeney, and Debajyoti Sinha. Beyond kappa: A review of interrater agreement measures. *Canadian journal of statistics*, 27(1):3–23, 1999.
- Huiman X Barnhart and John M Williamson. Modeling concordance correlation via GEE to evaluate reproducibility. *Biometrics*, 57(3):931–940, 2001.
- Huiman X Barnhart, Michael Haber, and Jingli Song. Overall concordance correlation coefficient for evaluating agreement among multiple observers. *Biometrics*, 58(4):1020–1027, 2002.
- Kristin P Bennett and Emilio Parrado-Hernández. The interplay of optimization and machine learning research. *Journal of Machine Learning Research*, 7(Jul):1265–1281, 2006.
- James O Berger. *Statistical Decision Theory and Bayesian Analysis*. Springer Science & Business Media, 2013.
- Austin J Brockmeier, Tingting Mu, Sophia Ananiadou, and John Y Goulermas. Quantifying the informativeness of similarity measurements. *The Journal of Machine Learning Research*, 18(1):2592–2652, 2017.
- Josep L Carrasco and Lluís Jover. Estimating the generalized concordance correlation coefficient through variance components. *Biometrics*, 59(4):849–858, 2003.
- Josep L Carrasco, Brenda R Phillips, Josep Puig-Martinez, Tonya S King, and Vernon M Chinchilli. Estimation of the concordance correlation coefficient for repeated measures using SAS and R. *Computer Methods and Programs in Biomedicine*, 109(3):293–304, 2013.
- Jacob Cohen. A coefficient of agreement for nominal scales. *Educational and Psychological Measurement*, 20(1):37–46, 1960.
- Olivier Collier and Arnak S Dalalyan. Minimax rates in permutation estimation for feature matching. *The Journal of Machine Learning Research*, 17(1):162–192, 2016.
- Ronán Michael Conroy, K Pyörälä, AP el Fitzgerald, S Sans, A Menotti, Gui De Backer, Dirk De Bacquer, P Ducimetiere, P Jousilahti, U Keil, et al. Estimation of ten-year risk of fatal cardiovascular disease in europe: the score project. *European heart journal*, 24(11):987–1003, 2003.
- Sara B Crawford, Andrzej S Kosinski, Hung-Mo Lin, John M Williamson, and Huiman X Barnhart. Computer programs for the concordance correlation coefficient. *Computer Methods and Programs in Biomedicine*, 88(1):62–74, 2007.

- Richard A Deyo, Paula Diehr, and Donald L Patrick. Reproducibility and responsiveness of health status measures statistics and strategies for evaluation. *Controlled clinical trials*, 12(4):S142–S158, 1991.
- Alvan R Feinstein and Domenic V Cicchetti. High agreement but low kappa: I. The problems of two paradoxes. *Journal of Clinical Epidemiology*, 43(6):543–549, 1990.
- Ronald A Fisher. *Statistical methods for research workers*. Edinburgh: Oliver and Boyd, 1925.
- Ronald Aylmer Fisher et al. A Mathematical Examination of the Methods of Determining the Accuracy of an Observation by the Mean Error, and by the Mean Square Error. 1920.
- Francis Galton. Typical laws of heredity. *Nature*, 15:492–5, 512–4, 532–3, 1877a.
- Francis Galton. Typical laws of heredity. *Proceedings of the Royal Institution*, 8:282–301, 1877b.
- Francis Galton. *Fingerprints*. Macmillan and Company, 1892.
- Carl Friedrich Gauss. *Briefwechsel zwischen CF Gauss und HC Schumacher*, volume 4. G. Esch, 1860.
- Godfrey Harold Hardy, John Edensor Littlewood, and George Pólya. *Inequalities*. Cambridge University Press, 1988.
- José Hernández-Orallo, Peter Flach, and Cèsar Ferri. A unified view of performance metrics: translating threshold choice into expected classification loss. *The Journal of Machine Learning Research*, 13(1): 2813–2869, 2012.
- Maurice G Kendall. A new measure of rank correlation. *Biometrika*, 30(1/2):81–93, 1938.
- Tonya S King and Vernon M Chinchilli. A generalized concordance correlation coefficient for continuous and categorical data. *Statistics in Medicine*, 20(14):2131–2147, 2001a.
- Tonya S King and Vernon M Chinchilli. Robust estimators of the concordance correlation coefficient. *Journal of Biopharmaceutical Statistics*, 11(3):83–105, 2001b.
- Gary G Koch. Intraclass correlation coefficient. *Encyclopedia of Statistical Sciences*, 4:213, 1982.
- Jean Kossaifi, Robert Walecki, Yannis Panagakis, Jie Shen, Maximilian Schmitt, Fabien Ringeval, Jing Han, Vedhas Pandit, Björn Schuller, Kam Star, Elnar Hajiyev, and Maja Pantic. SEWA DB: A Rich Database for Audio-Visual Emotion and Sentiment Research in the Wild. *IEEE Transactions on Pattern Analysis and Machine Intelligence*, 41, 2019.
- Klaus Krippendorff. Commentary: A dissenting view on so-called paradoxes of reliability coefficients. *Annals of the International Communication Association*, 36(1):481–499, 2013.
- Nicholas Lange, Stephen C Strother, Jon R Anderson, Finn Å Nielsen, Andrew P Holmes, Thomas Kolenda, Robert Savoy, and Lars Kai Hansen. Plurality and resemblance in fMRI data analysis. *NeuroImage*, 10(3):282–303, 1999.
- Joseph Lee Rodgers and W Alan Nicewander. Thirteen ways to look at the correlation coefficient. *The American Statistician*, 42(1):59–66, 1988.

- Erich L Lehmann and George Casella. *Theory of Point Estimation*. Springer Science & Business Media, 2006.
- Lawrence Lin, AS Hedayat, Bikas Sinha, and Min Yang. Statistical methods in assessing agreement: Models, issues, and tools. *Journal of the American Statistical Association*, 97(457):257–270, 2002.
- Lawrence I-Kuei Lin. A concordance correlation coefficient to evaluate reproducibility. *Biometrics*, pages 255–268, 1989.
- Lawrence I-Kuei Lin. Total deviation index for measuring individual agreement with applications in laboratory performance and bioequivalence. *Statistics in medicine*, 19(2):255–270, 2000.
- Matthew Lombard, Jennifer Snyder-Duch, and Cheryl Campanella Bracken. Content analysis in mass communication: Assessment and reporting of intercoder reliability. *Human communication research*, 28(4):587–604, 2002.
- Dan Ma, Vikas Gulani, Nicole Seiberlich, Kecheng Liu, Jeffrey L Sunshine, Jeffrey L Duerk, and Mark A Griswold. Magnetic resonance fingerprinting. *Nature*, 495(7440):187, 2013.
- Kenneth O McGraw and Seok P Wong. Forming inferences about some intraclass correlation coefficients. *Psychological Methods*, 1(1):30, 1996.
- Muhammed Murtaza, Sarah-Jane Dawson, Dana WY Tsui, Davina Gale, Tim ForsheW, Anna M Piskorz, Christine Parkinson, Suet-Feung Chin, Zoya Kingsbury, Alvin SC Wong, et al. Non-invasive analysis of acquired resistance to cancer therapy by sequencing of plasma DNA. *Nature*, 497(7447):108, 2013.
- Carol AE Nickerson. A note on “A concordance correlation coefficient to evaluate reproducibility”. *Biometrics*, pages 1503–1507, 1997.
- Satoshi Nishizuka, Lu Charboneau, Lynn Young, Sylvia Major, William C Reinhold, Mark Waltham, Hosein Kouros-Mehr, Kimberly J Bussey, Jae K Lee, Virginia Espina, et al. Proteomic profiling of the NCI-60 cancer cell lines using new high-density reverse-phase lysate microarrays. *Proceedings of the National Academy of Sciences*, 100(24):14229–14234, 2003.
- Vedhas Pandit, Nicholas Cummins, Maximilian Schmitt, Simone Hantke, Franz Graf, Lucas Paletta, and Björn Schuller. Tracking authentic and in-the-wild emotions using speech. In *Proc. 1st ACII Asia 2018*, Beijing, P. R. China, May 2018a. AAAC, IEEE.
- Vedhas Pandit, Maximilian Schmitt, Nicholas Cummins, Franz Graf, Lucas Paletta, and Björn Schuller. How Good Is Your Model ‘Really’? On ‘Wildness’ of the In-the-wild Speech-based Affect Recognisers. In *Proceedings 20th International Conference on Speech and Computer, SPECOM 2018*, Leipzig, Germany, September 2018b. ISCA, Springer.
- Vedhas Pandit, Maximilian Schmitt, Nicholas Cummins, and Björn Schuller. I know how you feel now, and here’s why!: Demystifying Time-continuous High Resolution Text-based Affect Predictions In the Wild. In *Proceedings of the 32nd IEEE International Symposium on Computer-Based Medical Systems (CBMS 2019)*, pages 465–470, Córdoba, Spain, June 2019. IEEE, IEEE.

- Vedhas Pandit, Maximilian Schmitt, Nicholas Cummins, and Björn W. Schuller. I see it in your eyes: Training the shallowest-possible CNN to recognise emotions and pain from muted web-assisted in-the-wild video-chats in real-time. *Information Processing and Management*, 57, 2020.
- Karl Pearson. Note on regression and inheritance in the case of two parents. *Proceedings of the Royal Society of London*, 58:240–242, 1895.
- Hui Quan and Weichung J Shih. Assessing reproducibility by the within-subject coefficient of variation with random effects models. *Biometrics*, pages 1195–1203, 1996.
- Paul R Rider. A survey of the theory of small samples. *Annals of Mathematics*, pages 577–628, 1930.
- Konrad Rieck and Pavel Laskov. Linear-time computation of similarity measures for sequential data. *Journal of Machine Learning Research*, 9(Jan):23–48, 2008.
- Fabien Ringeval, Björn Schuller, Michel Valstar, Roddy Cowie, and Maja Pantic, editors. *Proceedings of the 5th International Workshop on Audio/Visual Emotion Challenge, AVEC’15, co-located with MM 2015*, Brisbane, Australia, October 2015. ACM, ACM.
- Fabien Ringeval, Michel Valstar, Jonathan Gratch, Björn Schuller, Roddy Cowie, and Maja Pantic, editors. *Proceedings of the 7th International Workshop on Audio/Visual Emotion Challenge, AVEC’17, co-located with MM 2017*, Mountain View, CA, October 2017. ACM, ACM.
- Fabien Ringeval, Björn Schuller, Michel Valstar, Roddy Cowie, Heysem Kaya, Maximilian Schmitt, Shahin Amiriparian, Nicholas Cummins, Dennis Lalanne, Adrien Michaud, Elvan Ciftci, Hüseyin Gülec, Albert Ali Salah, and Maja Pantic. AVEC 2018 Workshop and Challenge: Bipolar Disorder and Cross-Cultural Affect Recognition. In *Proceedings of the 8th International Workshop on Audio/Visual Emotion Challenge, AVEC’18, co-located with the 26th ACM International Conference on Multimedia, MM 2018*, Seoul, South Korea, October 2018a. ACM, ACM.
- Fabien Ringeval, Björn Schuller, Michel Valstar, Nicholas Cummins, Roddy Cowie, Mohammad Soleymani, Maximilian Schmitt, Shahin Amiriparian, Eva-Maria Messner, Leili Tavabi, Siyang Song, Sina Alisamir, Shuo Lui, Ziping Zhao, and Maja Pantic. AVEC 2019 Workshop and Challenge: State-of-Mind, Depression with AI, and Cross-Cultural Affect Recognition. In Fabien Ringeval, Björn Schuller, Michel Valstar, Nicholas Cummins, Roddy Cowie, and Maja Pantic, editors, *Proceedings of the 9th International Workshop on Audio/Visual Emotion Challenge, AVEC’19, co-located with the 27th ACM International Conference on Multimedia, MM 2019*, Niece, France, October 2018b. ACM, ACM.
- M. Schmitt and B. Schuller. openXBOW – Introducing the Passau Open-Source Crossmodal Bag-of-Words Toolkit. *Journal of Machine Learning Research*, 18(96):1–5, 2017.
- Maximilian Schmitt, Nicholas Cummins, and Björn W. Schuller. Continuous Emotion Recognition in Speech – Do We Need Recurrence? In *Proceedings INTERSPEECH 2019, 20th Annual Conference of the International Speech Communication Association*, pages 2808–2812, Graz, Austria, September 2019. ISCA, ISCA.
- Oscar B Sheynin. Cf gauss and the theory of errors. *Archive for history of exact sciences*, 20(1):21–72, 1979.

- Patrick E Shrout and Joseph L Fleiss. Intraclass correlations: uses in assessing rater reliability. *Psychological Bulletin*, 86(2):420, 1979.
- Nigel C Smeeton. Early history of the kappa statistic. *Biometrics*, 41:795, 1985.
- Charles Spearman. The proof and measurement of association between two things. 1961.
- Roy T St. Laurent. Evaluating agreement with a gold standard in method comparison studies. *Biometrics*, pages 537–545, 1998.
- Gábor J Székely, Maria L Rizzo, Nail K Bakirov, et al. Measuring and testing dependence by correlation of distances. *The annals of statistics*, 35(6):2769–2794, 2007.
- Richard Taylor. Interpretation of the correlation coefficient: A basic review. *Journal of Diagnostic Medical Sonography*, 6(1):35–39, 1990.
- George Trigeorgis, Fabien Ringeval, Raymond Brückner, Erik Marchi, Mihalis Nicolaou, Björn Schuller, and Stefanos Zafeiriou. Adieu Features? End-to-End Speech Emotion Recognition using a Deep Convolutional Recurrent Network. In *Proceedings 41st IEEE International Conference on Acoustics, Speech, and Signal Processing, ICASSP 2016*, pages 5200–5204, Shanghai, P. R. China, March 2016. IEEE, IEEE.
- Michel Valstar, Jonathan Gratch, Björn Schuller, Fabien Ringeval, Roddy Cowie, and Maja Pantic, editors. *Proceedings of the 6th International Workshop on Audio/Visual Emotion Challenge, AVEC’16, co-located with MM 2016*, Amsterdam, The Netherlands, October 2016. ACM, ACM.
- Frank M Weida. On various conceptions of correlation. *Annals of Mathematics*, pages 276–312, 1927.
- Felix Weninger, Fabien Ringeval, Erik Marchi, and Björn Schuller. Discriminatively trained recurrent neural networks for continuous dimensional emotion recognition from audio. In *Proceedings of the 25th International Joint Conference on Artificial Intelligence, IJCAI 2016*, pages 2196–2202, New York City, NY, July 2016. IJCAI/AAAI.
- Cort J Willmott and Kenji Matsuura. Advantages of the mean absolute error (MAE) over the root mean square error (RMSE) in assessing average model performance. *Climate research*, 30(1):79–82, 2005.
- Zhengjun Zhang et al. Quotient correlation: A sample based alternative to pearson’s correlation. *The Annals of Statistics*, 36(2):1007–1030, 2008.
- Xinshu Zhao, Jun S Liu, and Ke Deng. Assumptions behind intercoder reliability indices. *Annals of the International Communication Association*, 36(1):419–480, 2013.